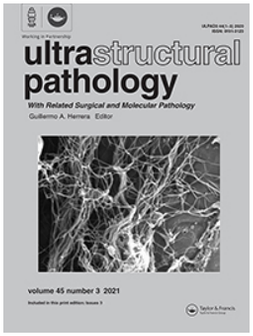

Ultrastructural Pathology

ISSN: (Print) (Online) Journal homepage: https://www.tandfonline.com/loi/iusp20

Leptin receptor defect with diabetes causes skeletal muscle atrophy in female obese Zucker rats where peculiar depots networked with mitochondrial damages

Jacques Gilloteaux, Charles Nicaise, Lindsay Sprimont, John Bissler, Judith A Finkelstein & Warren R Payne

To cite this article: Jacques Gilloteaux, Charles Nicaise, Lindsay Sprimont, John Bissler, Judith A Finkelstein & Warren R Payne (2021): Leptin receptor defect with diabetes causes skeletal muscle atrophy in female obese Zucker rats where peculiar depots networked with mitochondrial damages, Ultrastructural Pathology, DOI: 10.1080/01913123.2021.1983099

To link to this article: https://doi.org/10.1080/01913123.2021.1983099

Published online: 07 Nov 2021.

ULTRASTRUCTURAL PATHOLOGY
https://doi.org/10.1080/01913123.2021.1983099

Taylor & Francis
Taylor & Francis Group

Leptin receptor defect with diabetes causes skeletal muscle atrophy in female obese Zucker rats where peculiar depots networked with mitochondrial damages

Jacques Gilloteaux[a,b,c*], Charles Nicaise[b], Lindsay Sprimont[b], John Bissler[c,d], Judith A Finkelstein[c+], and Warren R Payne[e*]

[a]Department of Anatomical Sciences, St George's University School of Medicine, K B Taylor Global Scholar's Program at the University of Northumbria, School of Health and Life Sciences, Newcastle upon Tyne, UK; [b]Unité de Recherches de Physiologie Moleculaire (URPHyM) - Narilis, Département de Médecine, Université de Namur, Namur, Belgium; [c]Department of Anatomy, Northeast Ohio Medical University (Neomed), Rootstown, OH, USA; [d]Division of Nephrology at St. Jude Children's Research Hospital and Le Bonheur Children's Hospital, The University of Tennessee Health Science Center, Memphis, TN, USA; [e]Institute for Sport and Health, Footscray Park Campus, Victoria University, Melbourne, VIC, Australia

ABSTRACT

Tibialis anterior muscles of 45-week-old female obese Zucker rats with defective leptin receptor and non-insulin dependent diabetes mellitus (NIDDM) showed a significative atrophy compared to lean muscles, based on histochemical-stained section's measurements in the sequence: oxidative slow twitch (SO, type I) < oxidative fast twitch (FOG, type IIa) < fast glycolytic (FG, type IIb). Both oxidative fiber's outskirts resembled 'ragged' fibers and, in these zones, ultrastructure revealed small clusters of endoplasm-like reticulum filled with unidentified electron contrasted compounds, contiguous and continuous with adjacent mitochondria envelope. The linings appeared crenated stabbed by circular patterns resembling those found of ceramides. The same fibers contained scattered degraded mitochondria that tethered electron contrasted droplets favoring larger depots while mitoptosis were widespread in FG fibers. Based on other interdisciplinary investigations on the lipid depots of diabetes 2 muscles made us to propose these accumulated contrasted contents to be made of peculiar lipids, including acyl-ceramides, as those were only found while diabetes 2 progresses in aging obese rats. These could interfere in NIDDM with mitochondrial oxidative energetic demands and muscle functions.

ARTICLE HISTORY
Received 31 August 2021
Accepted 16 September 2021

KEYWORDS
Diabetes 2; skeletal muscle; atrophy; lipids; mitochondria; ceramide

Introduction

> We must always tell what we see. Above all, and this is more difficult, we must always see what we see. Charles Péguy (1873–1914).

Diabetes is a worldwide-distributed metabolic malady that afflict people with type 2 or non-insulin dependent diabetes mellitus (NIDDM), typically developed in aging adults. Nowadays, the rate of diabetes 2 is also increasing in all ages, including children and young adults, due to over-weight, unhealthy diet and physical inactivity. Diabetes 2 has been known since Antiquity[1] and the topic has been reviewed by an immense number of clinical care specialists in biomedical fields. Its impact on public health cost is surveyed by national and international organizations of medicine, because its metabolic alterations favors many other disabilities and pathologies leading to an excess of fatalities before age 70.[2–9] One of the etiologies is a defective adipokine leptin receptor.[10–12] The animal model that best matches human leptin receptor defect is the genetically obese Zucker rat[13–33] which progresses at an early age to diabetes 2 because, soon after weaning, young male and female rodents of the *fa/fa* (obese) strain manifest hyperphagia.[12] Thus, at young age, this rodent rapidly develops a clear phenotypic obesity due to leptin excess with hyperinsulinemia and insulin insensitivity. Consequently, these growing and aging rats undergo other endocrine entwined defects that favored multiple organ

CONTACT Jacques Gilloteaux jacques.gilloteaux@unamur.be; jgilloteaux@sgu.edu URPhyM - Narilis, Département de Médecine, Université de Namur, Rue de Bruxelles 61, Namur 5000, Belgium; Department of Anatomical Sciences, St George's University School of Medicine at UNN-School of Life Sciences, Northumbria Street, Drill Hall 013, NE1 8JG Newcastle upon Tyne, United Kingdom

[+]deceased

*JG and WRP dedicate this study to the late Dr F Norman Paradise, colleague, and colleague and mentor at the Northeastern Ohio Universities College of Medicine (now NEOMed), USA and to Dr Albert Claude, 1974 Nobel laureate, who reviewed JG doctoral thesis on muscle ultrastructure.

function's changes similarly to what one can find in most of the clinical progression in the human NIDDM in diabetes type 2.[13–33]

Even though the skeletal muscles encompass about 40% body weight and the tissue plays an important regulatory function in expenditure due to its functions in locomotion and metabolism,[34] it is only a very small number of ultrastructure reports that have been published about the human obesity and diabetes 2 skeletal muscles.[35–37] There, lipid depots but mitochondria functions seemed to have lastly delved on this last organelle in NIDDM [e. g. [37–46] but this focus topic is not without controversy.[47] Like in human diabetes 2, the obese Zucker rat skeletal muscle histopathology does not appeared strikingly changed from a normal muscle sample with light microscopy and, thus, has remained neglected insofar about its fine features with aging. These and other tissues would be also influenced by several defective leptin transduction signals, including endocrine secretions out of hypothalamus and peripheral tissues (e.g. ghrelin in the stomach lining; adiponectin, resistin from adipose tissues), [10,11,23–27] as well as of the thyroid glands.[29–31] Muscle tissues are potent targets for the iodinated hormones to stimulate mitochondrial metabolic expenditure and, thus, could provide some relief for diabetes progress through increased storage's anabolism[38,48–54] in addition to or accompanying recent medications,[55] including in this Zucker rat model.[56]

This report extends an early histochemistry study, complemented by some preliminary electron microscopy investigations as abstracts.[57,58] Altogether, our fine structure data further show that diabetes 2 accompanied by leptin receptor defect, induces some skeletal muscles (in this case, the tibialis anterior muscles) of old female diabetic rats to atrophy also caused by a progress in their defective innervation.[32,33] Moreover, the oxidative fibers cursory examination of its semi-thin sections appeared with ragged aspect and the fine structure of these revealed undescribed electron-contrasted interconnected depots, liposome-like components of endoplasmic contiguities and continuities with adjacent mitochondria outer membranes. Based on recent literature and other in vitro data, we can point out that those stored lipids and other electron contrasted components could include ceramides and metabolites, key impeding compounds of insulin and leptin sensitivity.[59–63] Yet, at the time of these investigations, a lack of funding and time made us not able to further identify and characterize these depots by markers and complementary techniques because the same oxidative fibers showed scattered damaged and lytic mitochondria as remnants out of 'mitoptosis,' instead of mitophagy.[45–47,64] Interestingly, some of the damaged organelles appeared to house or accumulate similar, unidentified electron contrasted materials and lipids. Finally, the highest number of mitolyses, including mitoptosis, without involving lipid-like content were revealed in the fast glycolytic (FG) fibers. Associated with NIDDM, would these organelle's eliminations be part of ambulatory weakness due to FG fibers developing defects with time, as in human? .[65]

Material and methods

Ethical concerns

The Institutional Animal Care and Use Committee (AAALAC) of the Northeastern Ohio Universities College of Medicine (NEOMed), Rootstown, Ohio approved all the experimental protocols (animal maintenance, experimentation, anesthesia, sacrifice and/or euthanasia procedures) of the Zucker rats by Dr J Finkelstein who used them for brain studies,[23,24] endocrine organs and peripheral nerves[29–33] and by Dr N F Paradise for cardiac functions.[61,62] We were allowed to also use the rat's remains to excise several other organs, including the tibialis anterior muscles, used for this investigation.

Animal care and tissue's collection

The obese Zucker (or fatty) female rats that have both recessive traits (*fa/fa*) while Zucker rats *Fa/?* were the lean rats. Both genotypes possible of lean Zucker rats (either *Fa/Fa* or *Fa/?*) due to their either dominant homozygous trait or heterozygous; there, mark '?' indicates the uncertain trait associated with the lean rat used in laboratory, as relying on its morphology, characteristic of 'lean' or at least heterozygous rats as noted in previous publications.[29–33]

Five female obese Zucker rats (fa/fa) (45 weeks of age, 584 ± 20.2 g) and five lean littermates (Fa/?) (271 ± 11.5 g) out of a colony of rats purchased from Charles River Laboratories (Raleigh, NC) derived from original stocks[13–15,21,23,24] were all maintained in a constant environment (22°C) with a reversed 12 h/12 h light/dark cycle because the same age groups were part of another experiment dealing with exercise. The cycle was reversed to facilitate better running performance as rats are nocturnal animals. Purine lab chow and water were available ad libitum throughout their care.

Light (LM) and transmission electron (TEM) microscopy

Histochemistry

While hearts were used for cardiac performance investigations[66,67] and necessitated fast dissections avoiding interfering anesthesia, these 45-week-old female rats, were sacrificed by decapitation. Three tibialis anterior muscles from lean and from obese female Zucker rats were excised for histochemistry, frozen by isopentane cooled in liquid nitrogen, and 10-µm serially cut sections at −25°C were incubated for Ca^{2+}-activated ATPase (E.C. 3.6.1.3) by the method of Guth and Samaha (pre-incubation at pH 10.4)[68] and for succinate dehydrogenase (E.C. 1.3.99.1) or SDH[69] as applied in other skeletal muscle investigations.[70–72] Reagents were obtained from Sigma Chemical Co (St Louis Mo). Measurements of muscle diameters were accomplished by measuring the widest diameter of each fiber profile in one direction, then at right angle to the first, and taking the average of both values using Song's technique[73] and an Apple morphometric program.[70–75]

TEM processing

The rat's corpses used for LM were rapidly perfused with 3.5% buffered glutaraldehyde solution (0.1 M Na cacodylate, pH 7.35, at room temperature for 15 min), as in[71] and the 3 contralateral legs, sectioned with tibialis muscles still in situ, were excised to undergo the same fixation that continued for 2 h at 4°C. Washed in buffered sucrose solution, segments of muscle specimens were thinned into muscle fiber bundles, postfixed in 1.5% aqueous osmium tetroxide solution and processed for transmission (TEM) electron microscopy after embedment in PolyBed epoxy resin (Polysciences, Warrington PA.). One-µm thick sections, stained by toluidine blue, were observed with an Olympus BX51 light photomicroscope (Olympus America, Melville NY) to select areas for ultramicrotomy. Ultrathin sections were collected on 50, 75- and 100-mesh hexagonal copper grids (SPI, West Chester PA), contrasted by uranyl acetate and lead citrate prior to be examined in a JEOL 100 S electron microscope (JEOL USA, Inc, Peabody, MA).

Statistical analyses

Statistical analyses were performed with GraphPad Prism (v 7.0) statistical software. Normal distribution of fiber size was evaluated using a Kolmogorov-Smirnov test. All data were expressed as means ± s.e.m. Two-tailed Mann-Whitney test was used to test for differences between lean (fa/fa) and obese (Fa/?) rats, with a significant difference set at $p < .05$. One-way Kruskal-Wallis ANOVA followed by Dunn's multiple comparison test was applied to compare between both rat's 3 fiber types (FG, FOG and SO). Similar quantitative comparisons have been done concerning mitochondrial damages and lipid depots in relationships with section's areas observed.

Results

Light microscopy (LM)

General histology

The LM surveys of the semi-thin sections, stained by toluidine blue, the muscle fiber profiles displayed diverse aspects of staining characteristics, allowing to recognized them as 3 main types, with their specific staining topography. A brief qualitative survey allowed to recognize that the whitish-stained were always the widest fiber profiles, likely being the fast glycolytic fibers, displaying an almost transparent orthochromatic aspect compared with oxidative fibers that were narrower than the first ones. Moreover, the strongest with toluidine stain ones were the thinnest, matching the SO type with histochemistry (see 1.b) and all FOG revealed

outskirts whose qualitative profiles revealed many longitudinally-oriented, elongated, narrow intermyofibrillar masses and thick subsarcolemmal (and perikaryal) accumulations of admixed orthochromatic and metachromatic contrast. This morphology aspects made the fibers to appear more of less serrated, seemingly 'ragged' according to the randomness plane of thin sectioning. All semi-thin sections revealed their fine muscle cross-striations. The endomysium, made of intercellular loose connective elements, is displayed as narrow gaps between muscle fibers where small blood vessels, mainly capillaries, can be revealed. (Figure 1(a-d)).

Histochemistry and morphometry

Following samples of obese and lean muscles stained by classic histochemical markers as fiber types, a cursory look made LM aspects of all the

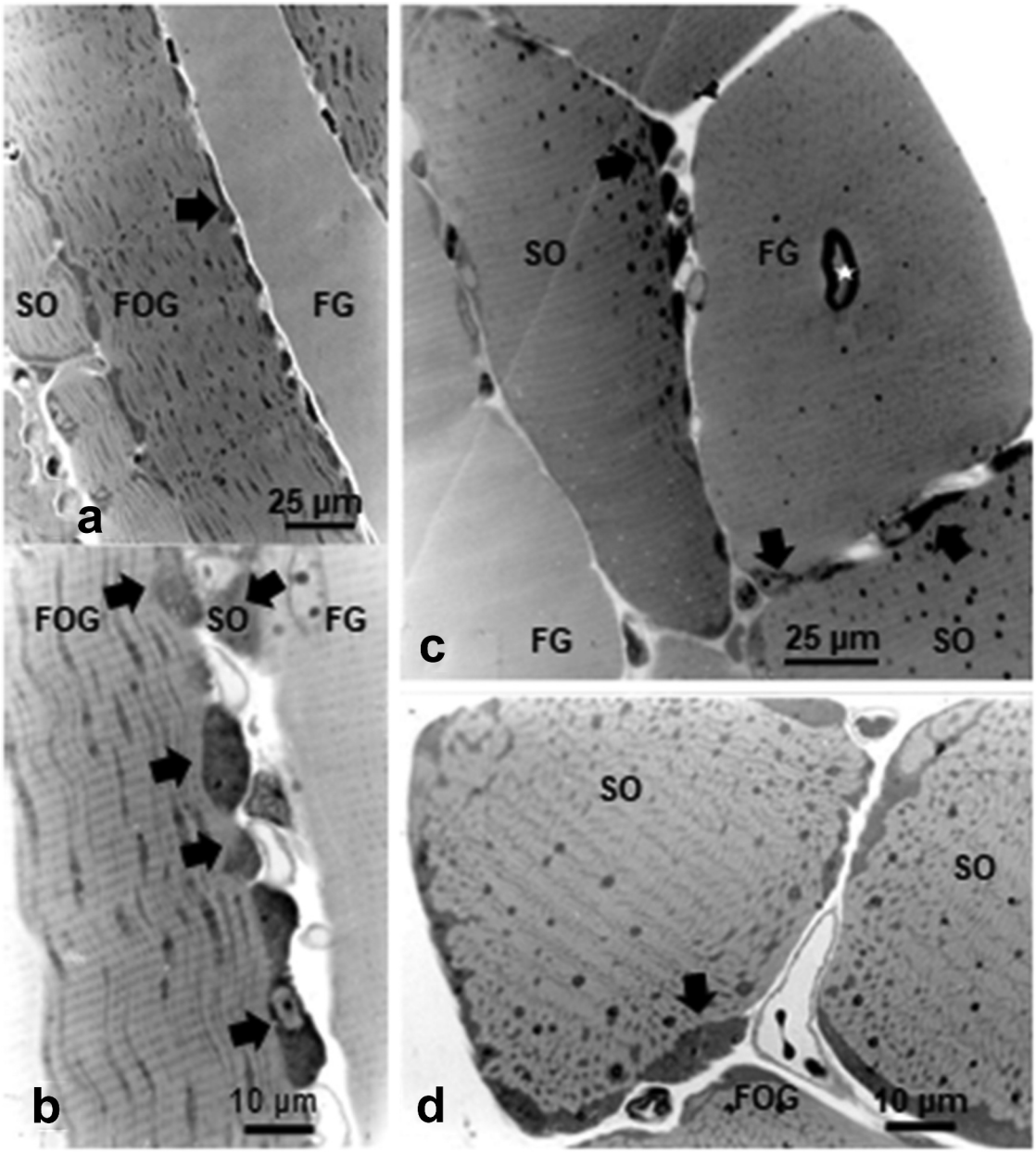

Figure 1. a-d: Pane of 1-µm thick longitudinal (a – c) and oblique cross-sections (b – d) of one 45 weeks old female obese Zucker tibialis anterior muscle, stained by toluidine blue. A cursory view reveals basophilic perikaryal and intermyofibrillar components in all the oxidative fibers, giving them a sort of 'ragged' aspect (black arrows). In overall, qualitatively, the muscle fiber diameters appeared as FG > FOG > SO types, whose diameter was verified quantitatively in (Figure 2(a-c)). b center displays a spot-fold artifact, not a central nucleus.

muscle fibers of the obese rats narrower than the lean muscle fiber of the same age female. Moreover, the histochemical markers and the histogram's comparisons between muscle fiber type measurement's distribution were illustrated (Figure 2(a,c)). There, the Kolmogorov-Smirnov tests, demonstrated with high significations that the quantitative measurements were normal

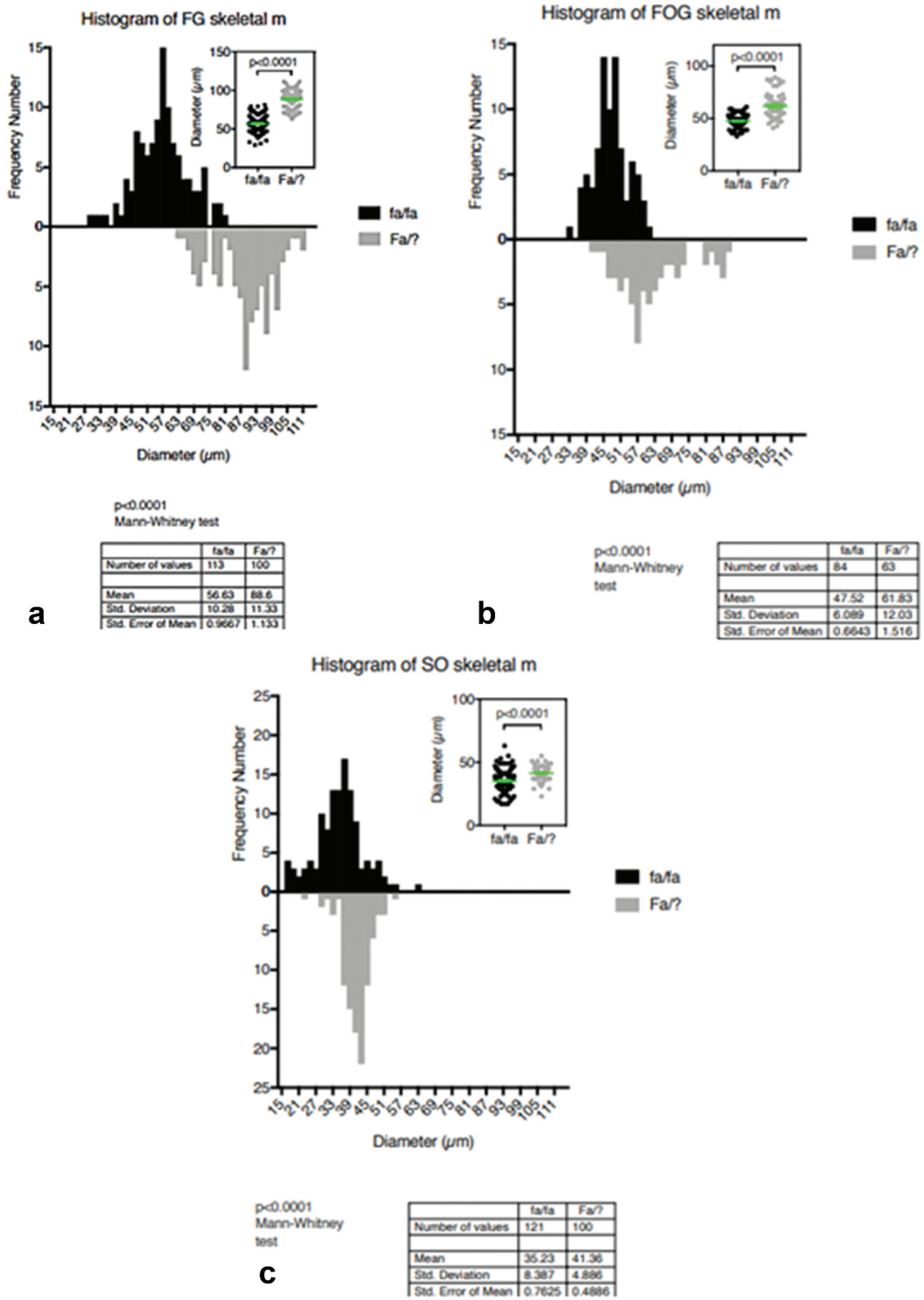

	fa/fa	Fa/?
Number of values	113	100
Mean	56.63	88.6
Std. Deviation	10.28	11.33
Std. Error of Mean	0.9667	1.133

	fa/fa	Fa/?
Number of values	84	63
Mean	47.52	61.83
Std. Deviation	6.089	12.03
Std. Error of Mean	0.6643	1.516

	fa/fa	Fa/?
Number of values	121	100
Mean	35.23	41.36
Std. Deviation	8.387	4.886
Std. Error of Mean	0.7625	0.4886

Figure 2. a-c. Comparative histograms of tibialis anterior muscle samples of Zucker obese and lean of the 45-week-old female rats and statistical comparisons indicate overall atrophy of the obese fiber types.

distributions ($p < .0001$) as well as the assumptions made with of histology qualitative aspects because SO or Type I fibers had 35.23 ± 8.387 µm in fa/fa (n = 121) vs 41.36 ± 4.886 µm (n = 100) with high significance (Figure 2(a)). The others, the fast oxidative glycolytic or intermediate type (FOG or type II A) in fa/fa measured 47.52 ± 6.089 µm (n = 84) vs Fa/? 61.83 ± 12.03 µm (n = 63) (Figure 2(b)) as well as the fast glycolytic type (FG or type IIB) revealed their narrow diameter in fa/fa 56.63 ± 10.28 µm (n = 113) to be still smaller than the ones of Fa/? having 88.60 ± 11.33 µm (n = 100) (Figure 2(c)). All the comparisons made between fiber types were verified with Mann-Whitney tests showing high significative meanings ($p < .0001$) Those comparisons between obese (fa/fa) and lean (Fa/?) fiber types of the tibialis muscles confirmed them to reveal and confirm the overall atrophy of the obese NIDDM muscles.

Transmission electron microscopy (TEM)

Out of LM 1-µm semi-thin sections (Figure 1(a)) of the muscle's samples, selected areas were used for ultrathin sections, as shown in the further figures. There, the 3 main skeletal muscle fiber types considered of the 45-week-old tibialis can be seen adjacent to one another, and even though already recognized with semi-thin sections, ultrastructure aspects made more comforting and new observations, especially about mitochondria and lipid deposits.

Subsarcolemmal and intermyofibrillar mitochondrial profiles

Accumulations of mitochondria profiles with adjacent osmiophilic deposits can be revealed in the outermost zones of the sarcoplasm and in the intermyofibrillar zones, also illustrated in all the Figures 4(a-c), 5(a,b), 6, 7, 8(a-d), 10(a,b), 11(c), 12(a) and 13(a). These accumulated mitochondria suggested and further confirmed that either the muscle profiles belonged to both oxidative fiber types, i. e. SO (type I) and FOG (type IIA) or fast fatigable or glycolytic as abbreviated FG, according to the histochemical profiles and fine aspects of this tibialis muscle fiber contents. The oxidative types have accumulations of the organelles but, especially, the FOG fibers would recall those described in muscle pathology as 'ragged.' However, if most of them do not seem to bear blemishes or altered microstructures at low magnification, the study of high magnification micrographs made us found peculiar scattered mitochondrial degradations with quasi obliteration or mitoptosis throughout the three fiber types (Figures 3, 4(a-c), 5(a,b), 6, 7, 8(a-d), 10(a,b), 11(c), 12(a) and 13(a) and Table 1).

The lipid depots (LDs)

The osmiophilic structures revealed different morphologies and can be subdivided into two types: (i) spherical fatty deposits (SDs) and (ii) interconnected subsarcolemmal or liposome-like bodies (Ls).

The spherical depots (SDs)

Specifically, large spherical fatty deposits ranging from 0.5 to 1.3 µm in diameter were usually located adjacent to mitochondria, either and both the subsarcolemmal zones or aligned with mitochondria in the intermyofibrillar sarcoplasm that belonged to both SO and FOG fibers (Figures 4(a-c), 5, 8(a,b), 10(c), 11(a)); however, these were only rarely viewed in the FG fibers (Table 2; Figures 3(a), 9(a) and 12(a, b), Table 1). In this subsarcolemmal location, some showed a bizarre and surprising eccentric degradation accompanied by debris (Figure 4(b)). With these accumulated mitochondria, SDs contributed the peripherally located festoons found in the LM sections (Figure 1(a-d)) that rendered the oxidative fibers as 'ragged.' It is only at the highest magnifications that these spherical structures appeared as lipid droplets without limiting membrane or apparent lining structure (Figures 5(a,b), 10(c,d), 11(a)). Their content displayed a sort of centripetal gradient of electron contrast reaching a lesser electron pale core as an amorphous blurry or mottled aspect, caused by the thickness of the sample's fixation, processing and sectioning (Figures 8, 10(c), 11(a), 12(a) and 13(c,d)). When detected in the subsarcolemmal zones, SDs showed a more uniform, full contrast but slightly distorted by the crowding with either the adjacent mitochondria profile and/or of a myofibril as well as the location of the triads (Figure 5(a,b)); SD distorted shapes revealed a homoeomorphic topology (Figures 4(a-c), 5(a,b),

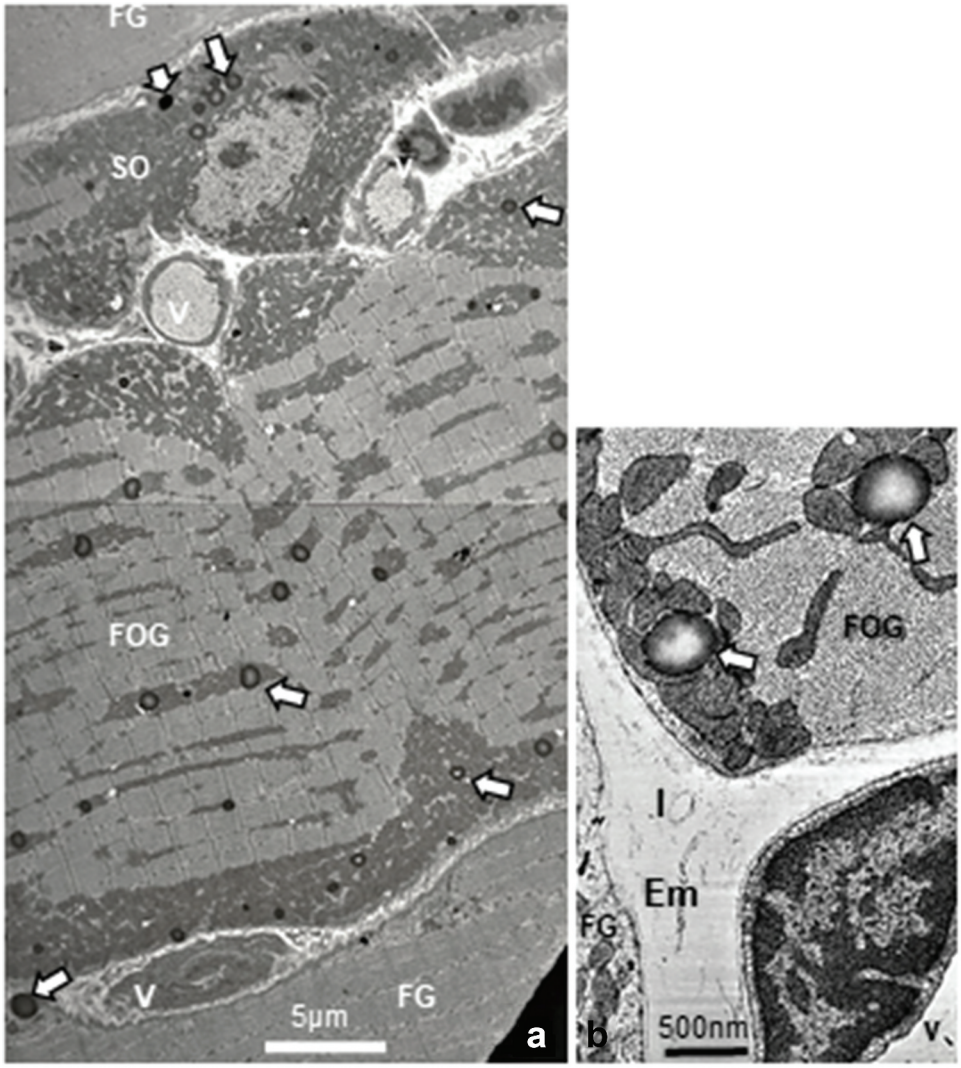

Figure 3. a-b: Pane of TEM aspects of 45-week-old obese female fa/fa tibialis anterior muscle showing parts of adjacent 3 main fiber types. Both SO and FOG fiber profiles typically contained mitochondria aggregates in the subsarcolemmal perikaryal and intermyofibrillar zones with large spherical lipid deposits (white arrows). FG fibers displayed only rare droplets (low left bottom arrow). b: Enlarged view of peripheral zone of an FOG fiber with spherical lipid depots (white arrows), adjacent to mitochondria. Em: Endomysium; FG: fast glycolytic fiber; v: blood vessel, l: lymphatic capillary.

Table 1. Comparisons between muscle tibialis sampled from obese (fa/fa) and lean (Fa/?) rats represented in Figure 2(a-c) as histograms.

Muscles	SO or Type I	FOG or Type IIA	FG or Type IIB			
n = 3	fa/fa	Fa/?	fa/fa	Fa/?	fa/fa	Fa/?
nb values	121	100	84	63	113	100
Mean Diameter	35.23	41.36	47.52	61.83	56.63	88.60
S.D.	8.387	4.886	6.089	12,03	10.28	11.33
s.e.m.	0.7625	0.4886	0.6643	1.5160	0.9667	1.1330

7, 9(a,b), 11(a), 12(a)). This deposit type is exceptionally found in the FG fibers (Figures 3(a),10(a), 12(a)). There, they were solitary and closely adjacent to the sarcolemma, often without a clear core.

The liposome networks (Ls) or interconnected subsarcolemmal deposits

Among oxidative fibers subsarcolemmal mitochondrial aggregates, other poorly recognizable deposits by LM aspects were only describable through fine structure aspects. Displayed as small lipid-like deposits, these Ls were highly and uniformly electron dense contrasted and their shapes varied; smaller than the SDs and found with the electron microscope as string-like accumulations recalling those of liposomes as lined by poorly-recognized lining membrane. Only found to the narrow perikaryal and sub sarcolemmal zones of the muscle fibers, their

Table 2. Obese female Zucker rat tibialis anterior muscle: mitochondria and spherical lipid deposits from 55–65 nm thick section's micrographs.

Skeletal muscle fiber types	SO fibers n = 3	FOG fibers n = 3	FG fibers n = 3
Surfaces of the illustrated fiber sections in μm^2	40	2100	250
	250	20	300
Total Section (µm2)	525	1250	90
	815	3370	740
Mitochondria			
Mitoptosis nb per total nb	10/123	5/86	6/25
mitochondria profiles in the	3/ 98	3/65	3/15
muscle fibers	15/269	15/365	8/15
Total nb mitochondria	490	516	55
Total nb mitoptoses	28	23	17
% Mitoptoses	5.71	4.45	30.90
Spherical Lipid Deposits (SDLS)			
Subsarcolemmal	1	1	1
SDLs nb	2	0	1
Total nb	1	3	1
Total Section's area (µm2)	4	4	3
% total Section	3.2005	3.1416	0.75
	1.5707	0.0932	0.0099
Intermyofibrillar	9	29	0
SDLs nb	12	4	0
Total nb	20	34	0
Total Section (µm2)	41	67	0
% total Sections	32.2014	52.6218	0
	3.9510	1.5614	0
Total section of SLDs (µm2)	35.4019	55.7634	0.75
% total Section	4.3438	1.6547	0.0993

n = number of muscle micrographs; nb: number; S: Surface section's measured.

fine structure features revealed them as if initiated near or by the small Golgi zones to form Ls (Figures 7, 10(a,b)). They also displayed interconnected oweverclumps of various shapes (Figures 6, 7, 9(a,b), 10(a)). With higher magnifications, Ls revealed a unit membrane lining with crenate aspect (Figures 6, 8(c,d)). In some oblique or tangential sections, the electron micrographs made up them of some aligned, interconnecting circular channels along their lining membranes, including those that contacted the outer membrane of the mitochondrial envelope (Figure 8(a-d)). In some cases, Ls were noted with a sort of hexagonal profile (Figure 8 (d)) among a filled to swollen homeomorphic endoplasm network (Figure 8(b)). Therefore, these Ls differed from the aforementioned SDs, those lacked lining membrane. In addition, the network of smooth endoplasm structures with electron contrasted content associated with the outer membrane's of the mitochondria envelopes through linkages or blunt conduits in continuity and their dense content of the intermembrane space, the inner membrane and the mitochondrial matrix (Figures 6 and 9(b)). Enlargements of some parts revealed in Figure 8(e,f) provide further details of the crenated lining of the Ls and its reticulum-containing complex that appeared to demonstrate elongated channel-like, resembling those found in vitro and in vivo, with lipids and phospholipids enriched by ceramides.

Mitochondria degradations and mitoptoses

Throughout all the muscles of the obese adult female Zucker rat, many of the mitochondria profiles showed either compacted matrices or with blurry aspects of matrices under high TEM magnifications in SO and FOG fibers (Figures 4(a-c), 7, 8(a,b), 9(a,b), 11(a-c)). Some others also showed scattered damage, and remnants of them. The damaged organelles were either swollen (Figure 4(a)) or both in part swollen and degraded (Figures 4(a), 5(a,b), 7, 8 (a), 9(a), 10(a), 11(a-c)) as well as entirely obliterated from the muscle fibers (Figures 11(a-c), 12(a-e)). Even with the small number of fibers illustrated throughout the illustrations collected of this report, we evaluated the ratios of mitochondria profiles degraded were most numerous in the FG fibers compared with both oxidative SO and FOG ones (Figures 12(a-d), 13(a-e); Table 1). In damaged organelles, inner membranes and cristae were still recognized within but in peculiar aspects, as illustrated by the pane of Figure 10(a-d), the mitochondrial remnants appeared as irregular morsels associated with electron dense droplets with a somewhat concentrically-aligned deposits as tiny electron dense deposits or granule-like with an accumulated centripetal-like pattern in the spaces made by the swollen or partially deteriorated mitochondria Internum or matrix (Figures 10(a-d), 11(a) and 14).

Endomysium

Most of the muscle fiber's basal laminae seemed to lack or were free from other typical

components of the basement membrane, i. e. collagen fibers of the endomysium, save

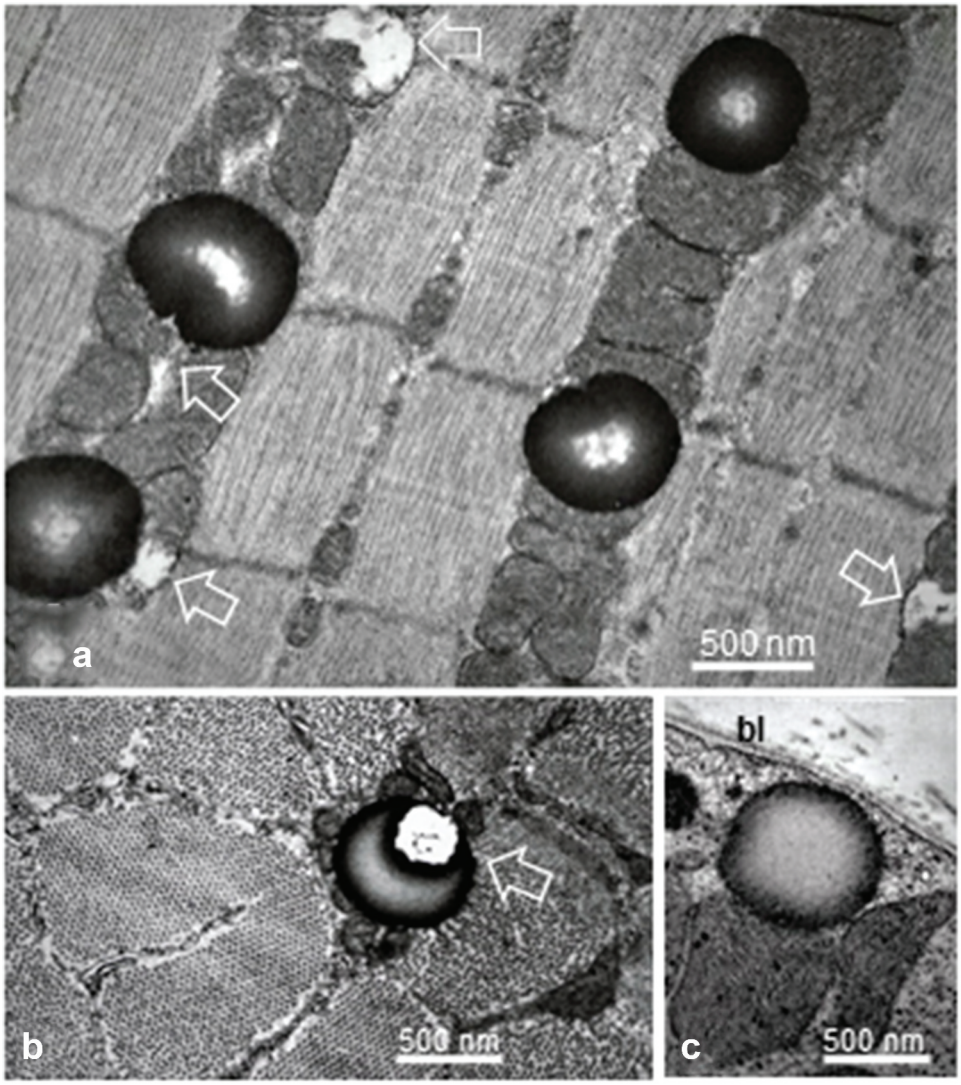

Figure 4. a-c: Enlarged spherical lipid deposits (SDs) located in intermyofibrillar location found in all SO or FOG fibers, among the rows of adjacent mitochondria as well as rare in subsarcolemmal position (c) and seldom found in FG fibers. White open arrows indicate damaged and degraded mitochondria throughout a and c. in b, a puzzling, eccentric fatty degradation between SD with mitochondrion. Note the centripetal gradient of oxido-reduced osmium contrast of all SDs. bl: basal lamina.

when muscle fibers were distant of less than 1-µm intercellular gap (Figures 5(a-c), 9(a,b), 10(a), 12(a)). Blood and rare lymphatic capillaries were often detected in the intercellular spaces.

Discussion

The *fa/fa* Zucker rats

Obvious somatic differences contrast the obese Zucker rats from the lean Zucker rat or any other lean 'strains' of laboratory rats, whether male or females due to their stooped posture and size, at rest, they bare their excessive weight. Furthermore, anesthetized, the huge adipose reserves made the rodents expand to appear as sorts of thick quiches.[9–12] Following the discovery of leptin, a product of secretion by the adipose cells, enterocytes and probably other unknown cells and tissues that influenced multiple CNS neurocrine centers and modulates other tissue's functions [20–33,54] including antidiabetic effects.[9–11] However, born without adequate leptin receptors,[12–14,17–20] these rats are driven by gluttony and undergo diabetes 2. Both male and female rats showed the same pattern of NIDDM ensued defects.[12–33]

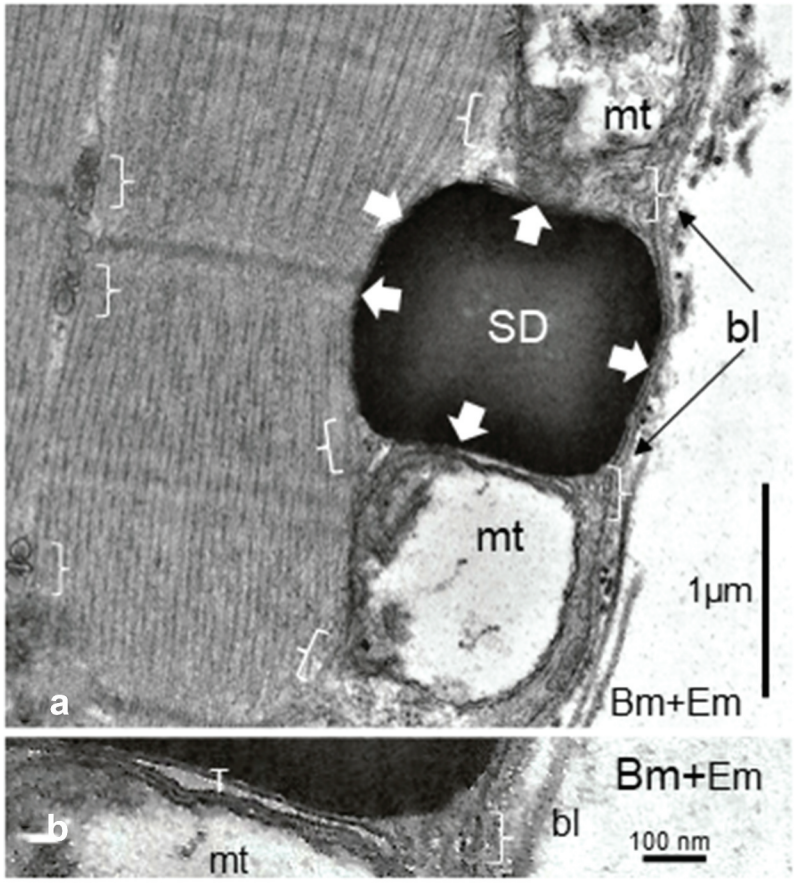

Figure 5. a-b Female Zucker FG tibialis muscle. a: SD deposit enlarged in the subsarcolemmal zone to view its inherent deformations (white arrows) caused by its adjacent muscle fiber substructures: sarcolemma, adjacents T-tubule (T), damaged mitochondria and myofibril. This later one also displayed a 'compressed' aspect, centered at and around its Z disc intersarcomere zone. Brackets: triad structures, including those displaced by deposit; bl: basal lamina; mt: mitochondrion. B: Enlarged aspect to verify the absence of membrane lining of the SD but T-tubule and part of mitochondria envelope are there, recognized. bl: basal lamina; Bm: Basement membrane; Em: endomysium.

Skeletal muscles and muscle fiber types

Skeletal muscle investigations have been achieved with animal models, invertebrates and vertebrates, including humans, through biopsies of patients and volunteered athletes. These abundant investigations allowed to comprehend both structure and functions of this bodily tissue, in deciphering its contractile fine machinery that the tissue has adapted with the skeletal frame for posture and locomotion e. g.[35,72–81] Out of these studies, using histochemical methods, at first, with toluidine blue alone[71,82] and, based on the intensity of staining at different pH levels, muscle fibers among muscles have been classified into 3 types, using myofibrillar ATPases and other mitochondrial dehydrogenases activities (such as succinic dehydrogenase (SDH)[49,68–72,74,75,83–89]; they provided a simple terminology as the SO (low ATPase, high SDH), FOG (high ATPase, high SDH) and FG fibers (high ATPase, low SDH). Ultimately, other studies subdivided human skeletal muscle tissue into seven human muscle fiber types, identified by myosin ATPase histochemical staining, from the slowest to the fastest ones: types I, IC, IIC, IIAC, IIA, IIAB, and IIB whose number's sequence corresponded from the 'red' or most 'oxidative' fibers (type I) to the most 'white' or 'glycolytic' ones as labeled IIB and, anatomically perceived from the most to least anatomical crimson tones corresponded to their relative content in myoglobin and mitochondria loads and activities.[49,80–89] Further refined biochemical techniques made ultimately 9 subtypes of the muscle fiber types to be recognized.[86–90] However, the adjacent subtypes tended to transiently convert into one another each other or to a main

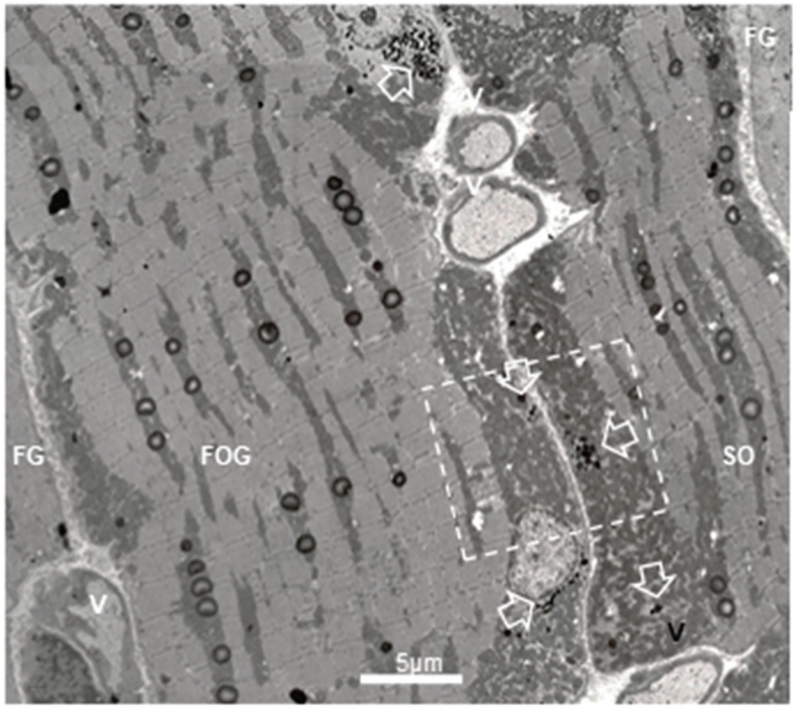

Figure 6. TEM montage pane of ibialis anterior muscle of obese female Zucker rat showing adjacent FG, FOG and SO fibers where a square indicated the field further enlarged in (Figure 7). White open arrows mark interconnected liposomes, only located in the subsarcolemmal and perikaryal muscle zones; rare SDs are also viewed. V: blood vessels.

functional 'type' according to the stimulated gene's expression(s) triggered after endurance and/or resistance training, with hypertrophy differences.[80,85,88] These can be used only for specialized study. However, these subtypes for any given muscle can be grouped differently by different researchers which created confusions between of published data comparisons. Thus, as cited and commented in several recent reports, most studies do not use these refined fiber types for making easier common ground of understanding between publications and categorize all muscle fibers into the 'original' three main fiber types.[68–70,83,84,89–95] Meanwhile, muscle genetic and histochemistry analyses demonstrated homologies between human and rodents e. g. [85–87, 89–94] and electron microscopy studies verified histology and fine structural homologies between rodents and human muscle fiber types [34,35,77–79,80,81,88–90, 92, 95–98]

The atrophy of the tibialis anterior muscle

As we followed the most common usage, we here reported about: (i) slow-twitch oxidative or type I (abbreviated SO), (ii) fast-twitch oxidative or type IIA (FOG) and (iii) fast-twich or type IIB (FG for 'fast glycolytic' or 'fast fatigable glycolytic') muscle fiber types. The rare, subtypes IIC, IIAC and IIAB were not even tried to be detected by special labelings, making less than 0.5% in this hindleg tibialis muscle. One has added to our initial reports about the obese Zucker rat muscles[57,58] and comforted other data on the same muscles where exercise physiology experiments were compared between male and female Zucker rats[99–102] and those about the same muscle without considering all 3 fiber types[93,103–110] by finding obese tibialis muscle fiber size demonstrated atrophy for all fiber types, 14.82% for SO fibers, 23,14% for FOG fibers and 24,79% for FG fibers respectively when compared to lean tibialis muscles whether in Zucker strain or other laboratory rats.[70,99,102,110–113] Overall, the obese Zucker muscle measurements found in this study supplemented other's data, such as those of poor incorporation of radiolabelled precursors,[112] reflected by decreased DNA and RNA contents,[113,114] likely hampered by deficient hypothalamo-hypophyseal signaling secretions caused by

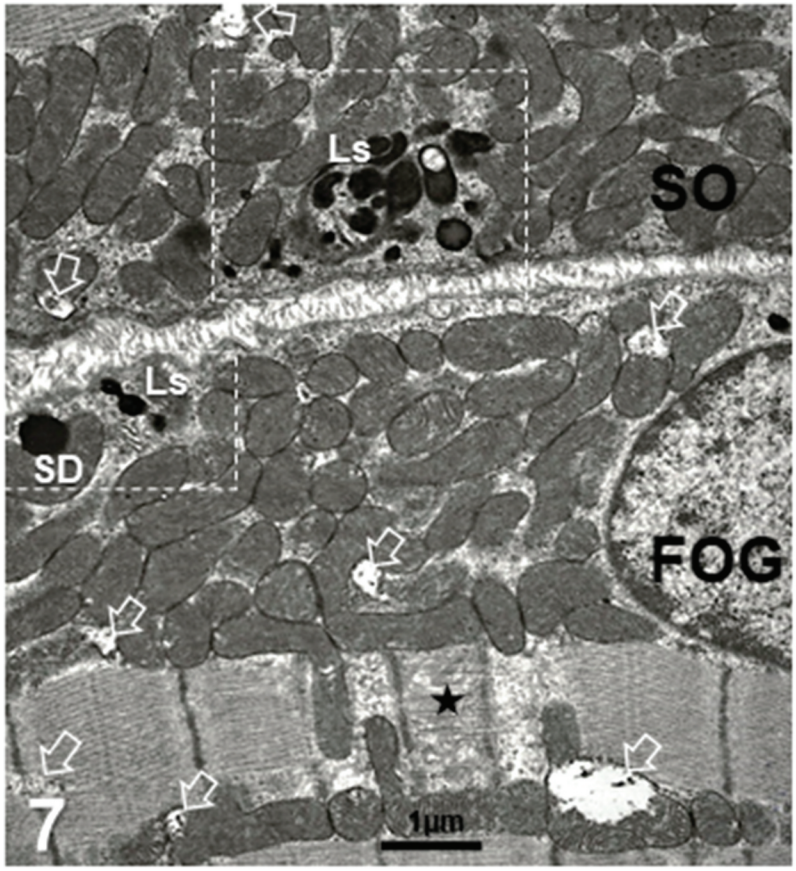

Figure 7. Ls and a single spherical deposit deposit in both SO and FOG fibers of an adult female obese Zucker rat (surrounded by broken rectangles whose enlarged views are displayed in (Figures 8(a) and 10(a-b)). Both fiber types contained mitochondria aggregates with a few degraded as marked with open arrows.

central leptin receptor defects, such as that of somatomedin (IGF-1), growth hormone (IGF-2)-[10,22–31,99,112–116] and still unknown factors, such some impeding bone[117] and insulin signaling and functions,[99–102,118,119] favoring thyroid gland changes[25,29–33,120] and poor vascular supply as parts of the defective muscle homeostasis ([108] vs [119,121,122]) and muscle atrophy that were also found in human diabetes 2.[123–125] This syndrome can be improved by exercise.[123] All the aforementioned data, including those of muscle, can also worsen with age in human cases[126,127] and the associated insulin resistance further increased by such sarcopenia.[125] The found muscle atrophy of the Zucker rat can be further comforted by a progression of tibialis nerve demyelination damages reported earlier, at younger age, where metabolites of sphingomyelin have been hypothesized, disrupting the myelin architecture [32,33]; see paragraph 4.b.

Skeletal muscle fine structure and diabetes obesity

Surprisingly, in human, only scarce but old studies have dealt with biopsies about fiber types[35–37,95–97,126,127] and after exercise[35,80,95,126,128] and too few about diabetes 2 [36,37] but included or based studies with only biochemistry aspects[7–9,125–129] even though utrastructural aspects would bring imagery resolution about crucial interpretative cell changes to verify and interpret some metabolic changes, like in many other tissues. A search through several specialized texts relevant to muscle defects confirmed this lack of human and animal ultrastructure data i. e. [130–135] Finding obesity-linked atrophy of the fiber types and serrated fringes of the oxidative fibers made us to further analyze fine features of the muscle samples with electron microscopy.

The distribution of both intramyofiber lipid depots LDs and SDs showed in our samples as well as those of young Zucker rats [99–102,112,113,136] corresponded to the known distribution in as

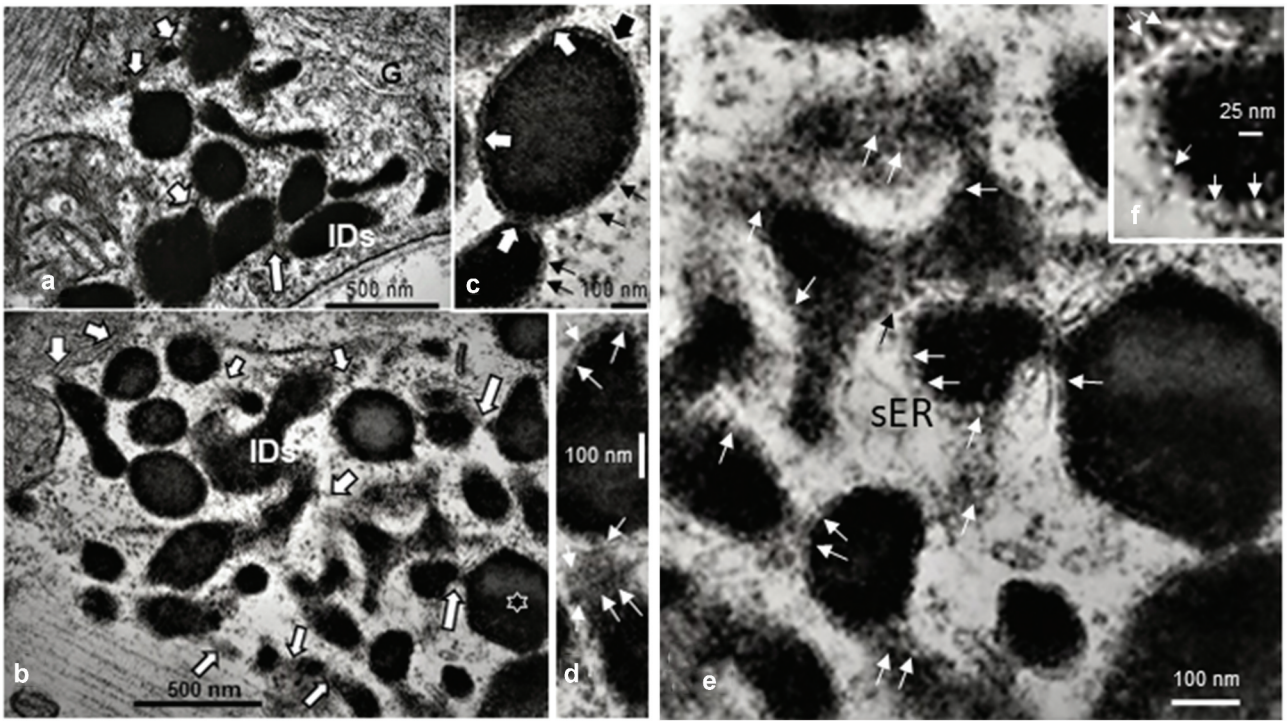

Figure 8. a-d: Example of liposome's aggregate (Ls) of 45-week-old female obese Zucker tibialis anterior muscle. a and b illustrate the numerous interconnecting bridges or channels appeared (white arrows) as a continuous reticulum contained the electron dense material that extended to the outer membrane of the mitochondria envelopes. In random sections, shapes of Ls varied in a sort of complex topology containing round to elongated ovoid into dodecahedron-like profiles (star) within the smooth endoplasmic reticulum. In c and d: Details of linings (in c, thick and white arrows) appeared and revealed a crenated aspect and, in d, further enlarged views of the same linings in oblique section formed sorts of circular, sieve-like aspect between encased pouch contents (thin white arrows) of similar size as those found ceramide-rich by others in vitro. g: Golgi; m: mitochondria. e-f: TEM enlargements of some parts of 8 b out of the previous pane revealed the crenated lining of the Ls complex (white arrows and a black on channel-like e). In f: micrograph further details demonstrated elongated channel-like, resembling those found in vitro, with phospholipids enriched by ceramides.

subsarcoplasm (SS) and intermyofibrillar (IM) lipid depots similar to those distributed in all typical mammal and humans[79–98,102,117,126–136] as well as those found in obesity and/or diabetes 2 cytopathology.[32,35,49,51,57,96,97,102,122,124–132] Other clinical studies have involved highly specialized imaging techniques, invasive or not invasive, and included the human tibialis anterior muscle as well as other muscles e. g. [112,113,126–128,136–142] with those of rodents, including the same Zucker rat model.[93,94,99–108,111–122,129,143,144] All confirmed the increased lipid depot distribution in diabetics and, surprisingly, the diabetic iris muscle was studied, even though, a smooth muscle.[145,146]

There, Zucker obese rat fatty deposit's distribution in fiber types was limited to red and white fibers[94,99,102,103,143] and other data showed there were no significative differences between human[34,36,45,49,51,80,96–102,134,136,143,144] with rodent's sex about muscle fiber type distribution.[35,93,103–107] One also can suggest that we found in old female diabetic rat's muscle ultrastructure could mirror unstudied old diabetic patients as a sort of incentive to pursue other human longitudinal studies. Additionally, leptin receptor models could also be created through gene knockout.

The lipid depots (LDs)

The LDs occurred in muscles like in many other tissues through coalescence from diffusion and endocytosis of extracellular heterogeneous hydrophobic dietary triglycerides, cholesterol metabolites and phospholipids sources.[35,49,126,129,147–150] These depots, as non-lined membrane droplets, in appearance unambiguous, with spherical profiles as those named here SDs, usually also accumulated small amounts of peculiar lipoproteins and

proteins, including several that hedge these fatty droplets as perilipins. In the lipid-rich matter, some enzymes linked to signaling and lipid synthesis, RNAs along with lipid-soluble toxicants have been detected.[147] LDs have been described as 'inclusions' in cytology or as secretory 'milk' products in mammary glands for offspring.[148,149,151,152] These intracellular droplets can located adjacent to mitochondria profiles, like in muscles[35,36,77–81,84,87–89,91,96–98,126,128,150,153–156] and, in large quantities in the adipose tissues, specialized for lasting storages for energy source triggered through β-oxidative stimuli or other neuro-hormonal signals, yielding maximal output of ATPs in muscles for contractility[35–37,49,50,52,147,154] or, pathologically, with changed content, to alter the Krebs cycle output.[38–48,51,53,154–157] In all our fine structure data, using a similar cacodylate buffered fixative and processing of muscle samples, as done in previous studies where the lipid droplet's content appeared typically electron-lucent in muscle tissues as in other reports about other cells[148,158–161] or of young diabetic muscles[36] and, without using imidazole buffers as in,[158–161] the peculiar electron contrasted content with central mottled part appeared to strongly indicate high levels of ethylenic bounded components comprising unsaturated lipids or metabolites that enabled fixation to undergo oxido-reduction process of osmium tetroxide into osmates[162–166]; there electron contrast could be further increased by ceramide moieties involving high C numbers among the depots[153,154,165] as also found in diabetes with biochemical analyses[63] and commented in the next 4.b and 4.b paragraphs.

Classic LM examination of biopsies[83,84,88,91,130–135] along with magnetic resonance spectroscopy analyses showed an inverse relationship between accumulated lipids in human skeletal muscle tissues and insulin sensitivity for sedentary and obese humans where muscle LDs tend to increase.[60,136–142,155–157,167–177] The LD's distribution in the obese Zucker rat skeletal muscle have concurred with those found in humans[34,36,45,49,51,80,96–102,134,136,143,144,178] and the obese female Zucker rats, like in both sex of mammals and human diabetes models, have oxidative muscle fibers always containing significant more SDs comparably to those rare, SDs of the fast glycolytic ones with LM and fine structure[145] whose measurements are summarized in Table 1 and in Figure 13(a,b). These findings comforted this rat diabetes 2, along with other functional aspects documented with light microscopy, biochemistry and histochemistry.[13,14,36,45,60,80,96–98,102,134,136,143,144] The clarification of the so-called 'athlete's paradox' facilitated in the understanding as to how skeletal muscles utilize lipids and made authors to revisit the idea that lipid uptake with excess depots in obesity and diabetes 2 could contribute to insulin resistance[39,40,45,54,56,150,152–158,167–170,179,180] due to muscle's reduced and repressed oxidative enzyme's activities, respectively.[150,168,179,180] On the opposite, endurance training favored lipid uptakes and if LDs increased, sometimes more than in obesity,[60,153,154] these stores became efficiently used by an adapted, heightened, aerobic anabolism[156,171–178,181–189] caused by upregulated transcriptional activities, such as those of mRNAs of the hormone-sensitive lipase (LIPE), intramyocellular fatty acid's transport via muscle fatty acid binding protein (FABP3), and oxidative phosphorylation (cytochrome c oxidase I), including those of the tibialis anterior muscle,[59,60,150,174] all boosted through high-intensity interval aerobic exercises.[150,173–178,181–183,190] It was with quite similar findings in rats,[191] including the Zucker rats.[192–195] Phosphorylation changes of the coating surface proteins or lipoproteins such as perilipin 5, associated with oxidative fibers, including other organelles and the LDs can be modified by specific exercises that would adapt and improve the human NIDDM syndrome [152–155,181,196] while perilipin 2 is mainly with glycolytic fibers, in lesser amount and mainly located around the very rare LDs of FG fibers.[154,181]

SDs as Ls with ceramides?

LD's fine morphology of the found SDs suggested the admixed presence of other lipid-soluble electron-dense containing highly ethylenic groups with polar compounds in these old female diabetic muscles that could perturb the energetic capabilities of the organelles, impeding the normal utilization of lipids by the fiber's mitochondria along with or as 'insulin resistance' in dealing mainly with oxidative fibers. Among these, least metabolically active

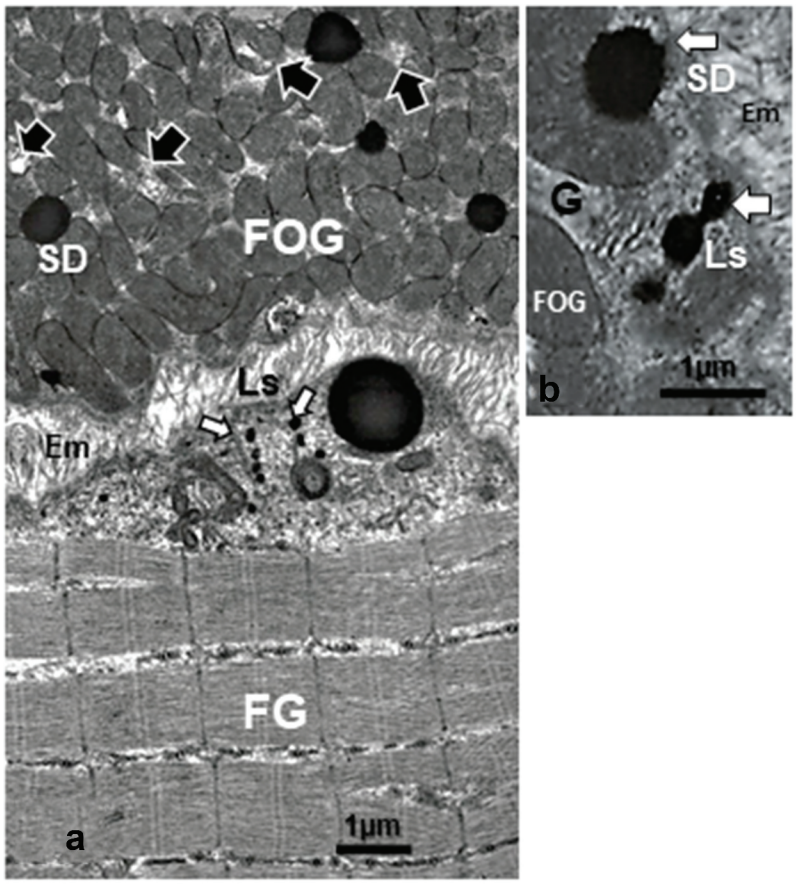

Figure 9. a-b: FOG and FG adjacent fibers of adult obese female Zucker rat tibialis anterior muscle. Note the FOG aggregate of mitochondria compared with the FG fiber (low part of 10A) devoid of such subsarcolemmal crowding but one SD showed closely adjacent to the sarcolemma. Both micrographs illustrate small aligned heavily contrasted strings of three vesicles in both fibers, marked by white arrows as Ls. A Golgi (g) zone could be involved with local endoplasm and process of capture and storage of these formed vesicles.

ones included long chain acyl-coenzyme As, diacylglycerol and ceramides.[39–46,59–63,191–195,198–202] Excessive lipid up taken caused by overfeeding and parts of the LDs, where ceramides originated from palmitate metabolism have lately received prominence after so much notices had focused on other lipids.[45,59–63,198–204] Ceramides in obese muscles could share multiple aspects in causing insulin resistance[62,205–207] through changing membrane surfaces,[208,209] displacing membrane rafts[206] with rearrangements of transmembrane channels[210] and changed other surface signalings[211] that could relate to the impeded mitochondrial respiration as 'resistance'[212] that can be reestablished by exercise, as discussed above.

An endoplasm reticulum filled excess amounts of inadequate metabolites, including lipids and ceramides as liposomes?

The sarcoplasm contains an endoplasmic reticulum highly specialized for fast ionic and energetic exchanger in muscles[35–37,77–81,83,84,97,98,130,131,213] and some part of it, like the sarcoplasmic reticulum, associated with ionic exchanges with myofibrils, could compartmentalize and specialize out of sarcolemma endocytosis and transcytosis, via Golgi apparatus and endosome-like, storage lipid sites. Obesity and hyperglycemia already make both increase in circulating shorter-chain saturated free fatty acids (FFA) that serve as substrates for and induce *de novo* ceramide synthesis[24,25,199–204] along with other complex lipids and cholesteryl esters captured by receptor-mediated endocytosis taken up from

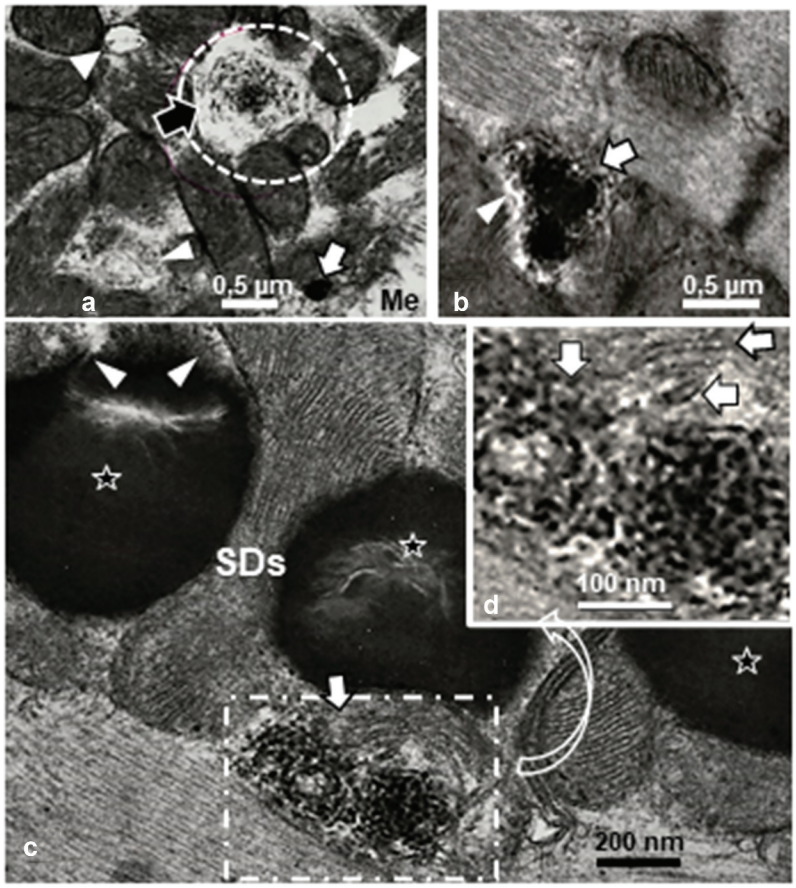

Figure 10. a – d: FOG and SO muscle fibers of adult obese female Zucker rat. Among the crowded intermyofibrillar mitochondria, degraded structures (arrowheads) bearing some concentric membrane whorls or stacks revealed what could be a filing by highly electron dense contrasted droplets ranging from 8–20 nm in diameter alongside those membranes (white arrows). d: Enlarged view of c demonstrates the centripetal-like trend of the aggregated deposits while becoming centrally coalescent and, thus, widened.

extracellular milieu (exiting circulation). Those can become parts of a reticulum of the endoplasm constructed with the subsarcolemmal Golgi apparatus (Figure 9(a,b)) into a membrane-enclosed lipids network of dynamic topology (as 'fixed' but illustrated in (Figures 6 and 8(e)). The string-like vesicles found in slow fibers resembled the chylomicrons found by others[214–216] – sometimes called liposomes – that resembled the same ones constructed artificially with double concentric amphiphilic lipid layers (phospholipids) that associate with water to form vesicles,[217,218] making 'nanoliposomes' to deliver medications,[217–220] including oligonucleotides (i.e., recent polyRNA vaccines against SARS-Cov 19). Ours are even more similar to those ceramides immunolabelled in keratinocytes.[221] Referring to our micrographs, accumulated liposomes enlarged by accretion and filled this swollen endoplasm network that acquire topologic variations of shapes, because of their corralled linings and as Ls, like in LDs, connected to the mitochondria oxidative 'furnaces.' Hence, those lipids enriched by complexed long-chain acyl groups, ceramides and their sphingosines 'escaping' autophagy through changes of perilipins[61–63,222] i. e. forming other electron- contrasted fine structures depots. Focusing about ceramides, the literature about them showed they not only overload the endoplasmic reticulum content but also its linings,[205–211,222–224] where membranes and intermembrane contacts in cross- and oblique sections showed peculiar crenated (<10 nm diam) to circular (10–25 nm in diam) formations in Figure 8 (c,e,f). These crenate aspects may relate to those reports that have not only detected membrane changes but also, in vitro verified channels made by accumulated ceramides including those found in mitochondria.[214,215,223,224] Whether or not ceramides or complex lipids, it is the first time, with

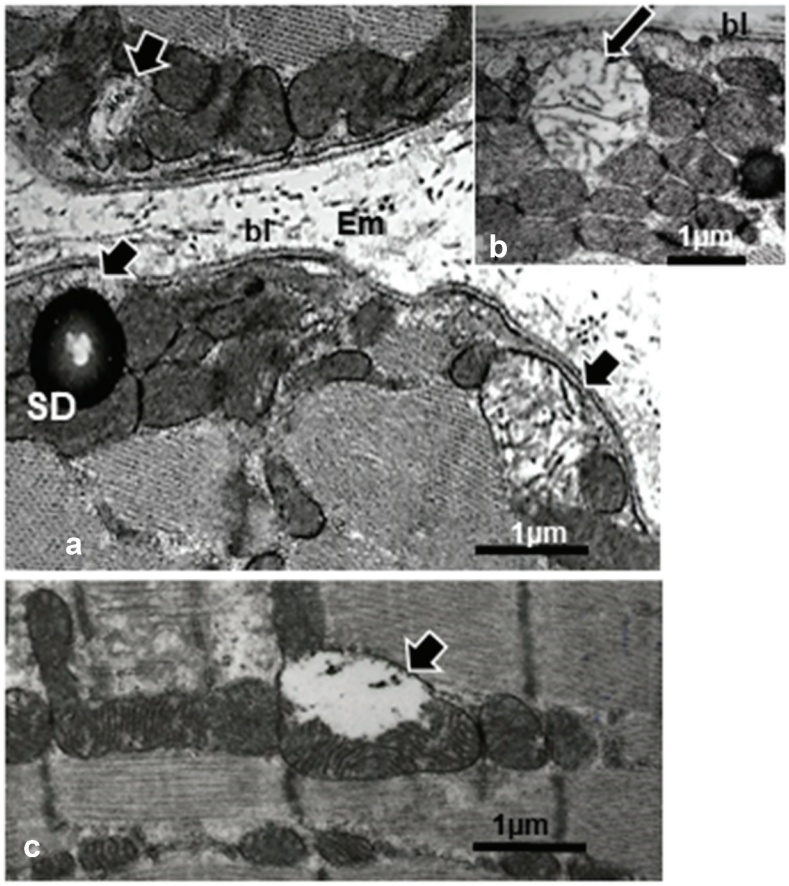

Figure 11. a-c: Typical mitolytic aspects or mitolysis in adult female obese Zucker rat tibialis anterior oxidative slow twitch (SO) and fast twitch or FOG muscle types. Profiles of sub-sarcolemmal (a-b) or intermyofibrillar (c) mitochondria revealed matrices either partially or entirely swollen-like degraded compared with other adjacent typical mitochondria profiles (white arrows). Highly contrasted SDs appear in both a and b. bl: basal lamina.

electron microscopy, that an 'endoplasm' displayed highly contrasted 'reticulum' or Ls network that reached and contacted the mitochondria outer membrane was detected in diabetes 2 muscles because LM aspects have not evidenced these structures yet.

Mitochondrial profiles and degradations as mitolyses and mitoptoses

As one noted in the above paragraph 4.c, the earliest reports dealing with human and animal model's investigations classically demonstrated the high content in mitochondria profiles along with lipid deposits in slow or oxidative fibers vs. those of glycolytic, fast twitch and fatigable. [35,36,77–81,64–83,97,98,130,131,225] However, token data collected about human and animal NIDDM/diabetes 2 muscle fine structure in specialized publications[35,36,126,128] could have been caused by LM poor resolution and marker's deficiency and, thus, may have reduced diabetes 2 interest with ultrastructure to befall focused on resolving metabolism. One also realized in our preliminary studies with LM alone that one disclosed atrophy and only glimpses of morphology alterations, similar to those that followed.[57,58] However, during the last three decades, molecular aspects have made so much strides and one would expect to provide interest for further longitudinal investigations in the TEM. Studies have clarified between the sub sarcolemma (SS) LDs and intermyofibrillar (IMF) LDs[153,154,220–222] along with specializations have been shown between them and the IMF and SS mitochondria due to proteomic and biochemical differences analyzed through mass spectrometry, because IMF LDs appeared to be the main fuel source for the IMF mitochondria that provide energy for adjacent myofibrils and sustained muscle contractility containing the highest levels of

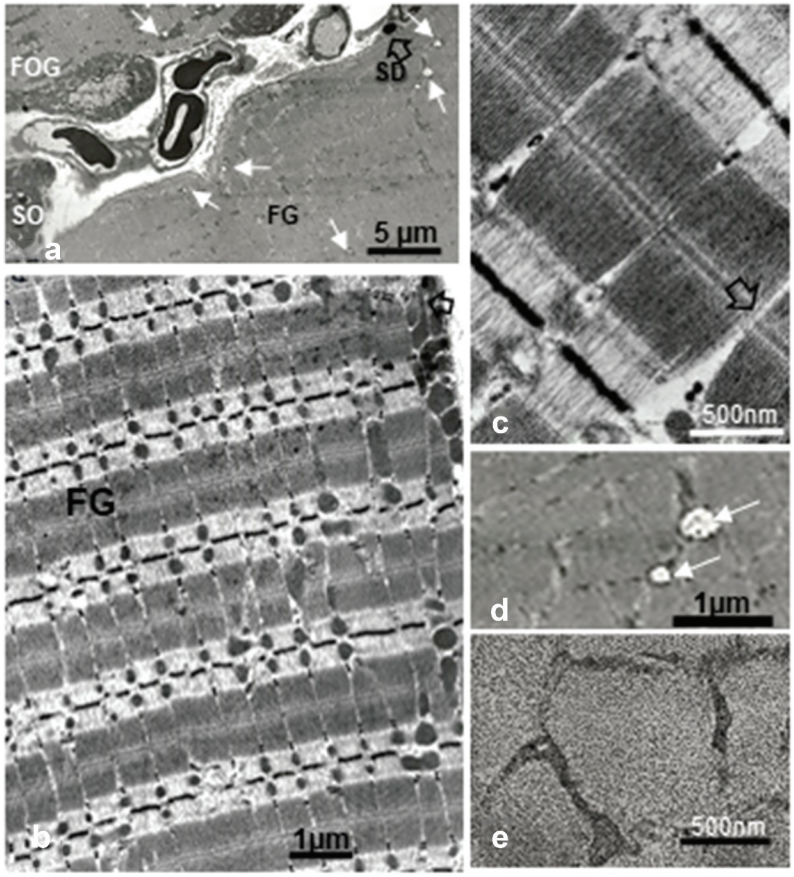

Figure 12. a-e: Obese female Zucker fast glycolytic (FG) muscle fiber ultrastructural aspects in cross, oblique and longitudinal sections. Typical myofibril architecture also showed throughout mitochondrial degradations as mitolyses or mitoptoses (small white arrows) and enlarged in d. These degradations occurred mostly within outermost regions of the myocytes. Notice throughout all the sections no glycogen aggregates (as in c, black arrows) showed in the intermyofibrillar sarcoplasm.

enzymes and phosphorylation proteins along with those respiratory chain complex while the SS LDs and mitochondria dealt with providing energetic demands for SS membrane related homeostatic and functions including those interactions-transports and dynamic exchanges of ions, metabolites of the adjacent endomysial space's.[14,60,66–81,153,220–224,226–228] Muscle fiber genome expression is also modulated by nerve influences, consistent with each fiber type and activity.[36,40,80,85,88,89,98,128,220–224,226–231] In the case of diabetes, palmitate metabolism yields ceramide and sphingosine compounds[59,61–63,198,199,211,229–231] and, probably, unlike of uninucleate cells, a pathway implicating reactive oxygen species (ROS) and reactive nitrogen species (RNS) in the organelles implicated, those located in SS locations and some IMF ones induce cytochrome c escape that activates an 'apoptotic'-like pathway that swerve into mitochondrial fission and/or degradation known as 'mitoptosis' instead of mitophagy.[45–47,64,202,231,232] However, as seen in all muscle fiber types, the lytic degradations which cause(s) is (are) unclear – maybe peroxidations – [45,46,231–234] damaged matrices or internum and the inner membrane of the envelopes while most of the external membranes were left preserved, rendered resilient due to their remodeling with ceramides and/or metabolites, providing diverse type channels[235–240]. The linings and extensions of the Ls membranes could be loaded with the same ceramides or sphingosines as we revealed circular infrastructures, described in paragraph 4.c. These mitochondrial partially or entirely executed with cavitation of their matrix[47,148] can also become sinks of overloaded complex lipids as suggested in tethering them in the lucent remnants as in Figure 10(a-c) and measurements seemed to have indicated that

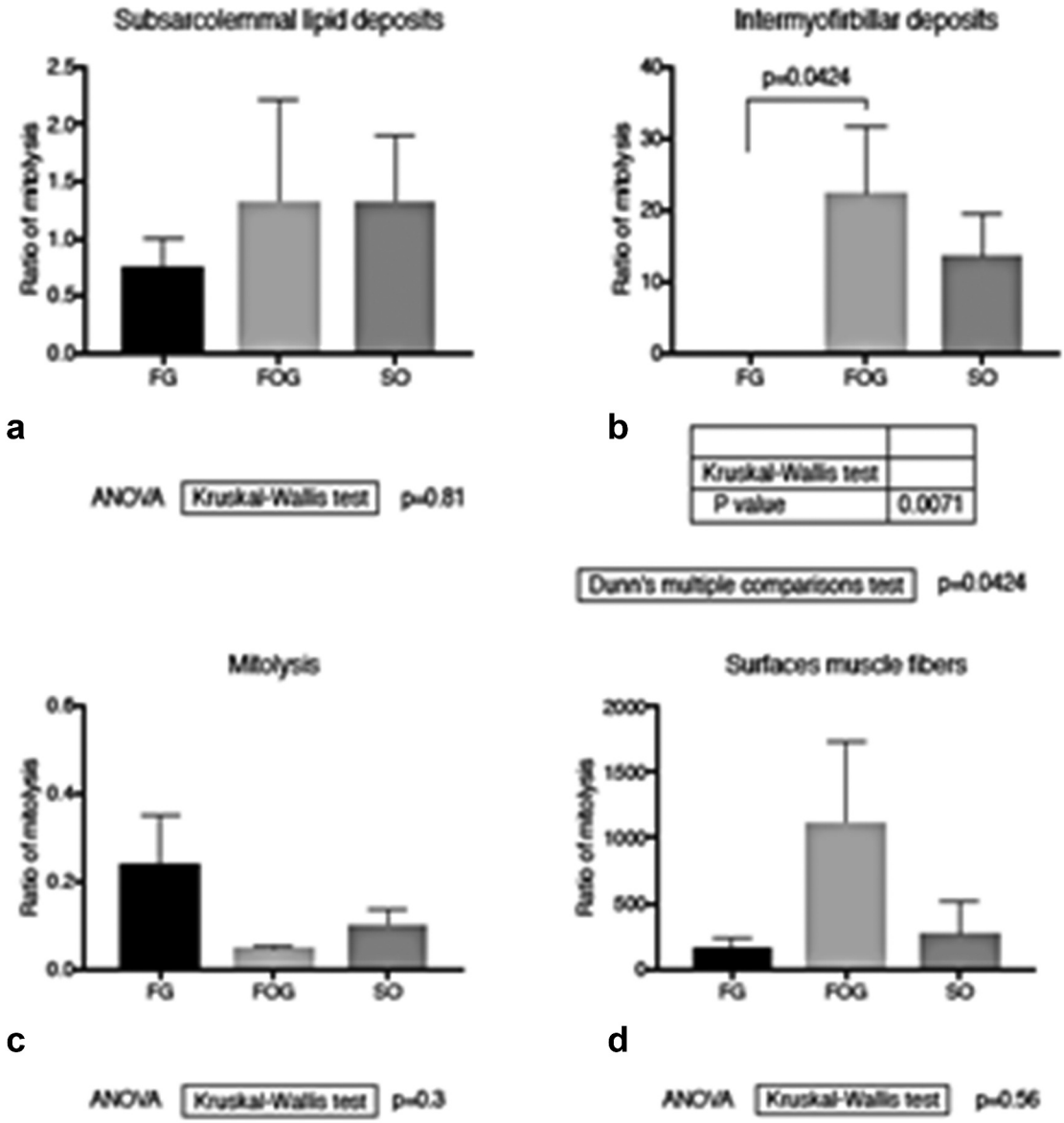

Figure 13. a-d: Comparative histograms from fine structure micrographic counts displaying more SDs in oxidative (SO and FOG) than FG fibers while none can be found FG fibers (a and b). In c: Mitolyses, including mitoptoses, are significantly more abundant in FG fibers than oxidative fibers. d: Surfaces of the 3 types of muscle ultrathin sections measured where a, b and c distributions were reported of the 45-week-old obese female Zucker rat tibialis anterior muscles.

for FG surfaces of sectioning measured, the number of mitolyses is significantly more important than in the oxidative fibers (Table 1 and Figure 13(c,d) where mitoptosis revealed only outer membrane of the envelope left. Could we hypothesize that, based on literature,[45–47,64,241] mitoptosis happened without apoptosis of the myocytes triggered by ceramides while myocytes were left to 'survive,' protected by their multinucleate structure that still control whatever can be in the diabetic syndrome mitochondria, with their altered their energetic capabilities.[199,200,212,213,225,228–234,237–243]

Diagrammatic representation in Figure 14 of the pane of (Figure 10(a-d)) suggesting the possibility of mitochondrion remnants as outer membrane, already natural 'sinks' for acylated lipids, gave in and yielded to become other lipid depots.

Conclusion and translational research considerations

Diabetes 2 as NIDDM syndrome condition of the female Zucker rat muscles showed to accumulate lipids and again demonstrated the validity of this

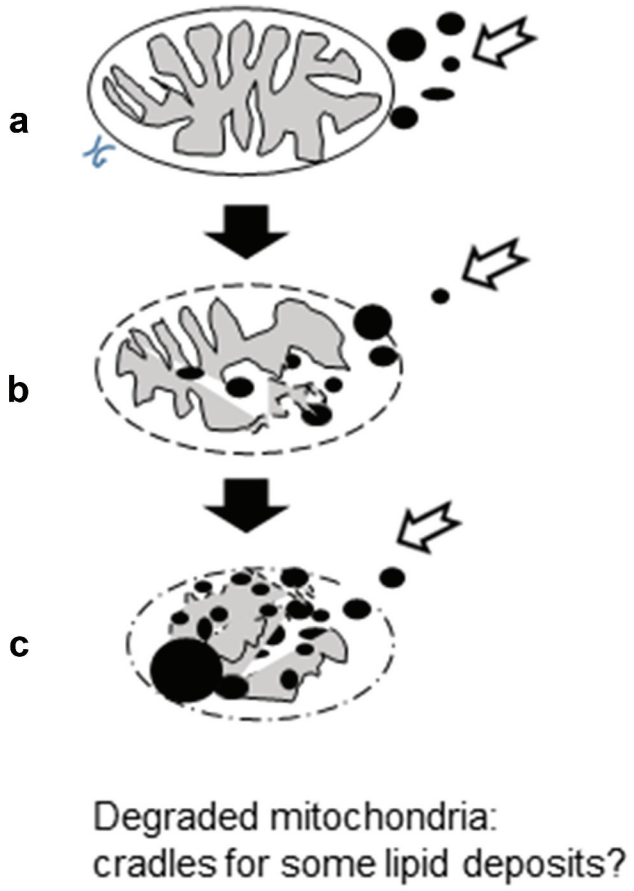

Figure 14. Diagrammatic representation suggesting the mitochondrion lytic remnant used as sink for diverse electron contrasted lipid and metabolites in oxidative muscle fibers.

rodent model to uncover some of the fine structure aspects associated correlated with peculiar metabolites depots[197] that could be involved in impeding sarcoplasm and mitochondrial anabolism, perturbing the insulin and other neurohormonal signals. Furthermore, our report concurred with the views of others[154,211] a that the regulatory mechanisms conferring lipid ceramide depositions[207] and utilization in skeletal muscle remain elementary and that more should be understood about musculature fine structure changes and gender along with aging in people afflicted by diabetes type 2, using interdisciplinary tools where fine morphology should be used along biochemistry markers for longitudinal investigations, including those of human biopsies, as it is done for other muscle diseases[244] Those could clarify functions and damages found as in Zucker rat model that may translate to further analyses of the human muscle's changes. These studies could bring into adjustments of the lipid-deficient or altered metabolism qualifying this public health syndrome and, could contemplate and assist as with the aging population with adjustment not only of seric glucose and carbohydrates nutrient's intake with new medications[10,245] but also, progressing with exercise and nutrients adaptations[37,51,246,247] along with further studies in rodents, whether with knockouts, and/or like with this rat model.[99,100,241,248,249]

Funding

This work was supported by JG and JAF Biomedical Grants USPHS Biomedical Grants USPHS-2-S 07/RR05806-06 and USPHS-S-O7 RR 058005-05 of Northeastern Ohio Universities College of Medicine (now Norheast Ohio Medical University or NEOMed), Rootstown, Ohio, USA.

Acknowledgments

JB made all the muscle's initial measurements with JG collecting ultrastructure data.[57,58] Data and bibliography were continued by JG while at with St George's University School of Medicine, Newcastle upon Tyne, KB Taylor Global Scholar's Programme, United Kingdom and Grenada WI and at the Université de Namur, Belgium with CN and LS for the text and the statistical analyses as well as with WRP, University Victoria, Australia, who studied data along with those involved with cardiac exercise.[66,67] The authors thanked St George's University School of Medicine, Newcastle upon Tyne, UK for the support in research activities and for defraying the Open Access costs of this original collaborative manuscript report.

Disclosure statement

No potential conflict of interest was reported by the author(s).

References

1. Karamanou M, Protogerou A, Tsoucalas G, et al. Milestones in the history of diabetes mellitus: the main contributors. *World J Diabetes*. 2016;7(1):1–7. doi:10.4239/wjd.v7.i1.1.
2. Horton ES. NIDDM - the devastating disease. *Diabetes Res Clin Pract*. 1995;28(Suppl):S3–11. doi:10.1016/0168-8227(95)01087-t.
3. Edelman SV. Type II diabetes mellitus. *Adv Intern Med*. 1998;43:449–500.

4. King H, Aubert RE, Herman WH. Global burden of diabetes, 1995-2025: prevalence, numerical estimates, and projections. *Diabetes Care*. 1998;21(9):1414–1431. doi:10.2337/diacare.21.9.1414.
5. Flegal KM, Carroll MD, Ogden CL, et al. Prevalence and trends in obesity among US adults, 1999–2008. *JAMA*. 2010;303(3):235–241. doi:10.1001/jama.2009.2014.
6. CDC Report. 2020. Estimates of diabetes and its burden in the United States. *National Diabetes Statistics Report*. 2020; 1–32.
7. Galan N. Diabetes statistics 2021. Single Care Team. 2021. https://www.singlecare.com/blog/news/diabetes-statistics/2021 .
8. Montague CT, Farooqi S, Whitehead JP, et al. Congenital leptin deficiency is associated with severe early-onset obesity in humans. *Nature*. 1997;387 (997):903–908. doi:10.1038/43185.
9. Hayden MR, Banks WA. Deficient leptin cellular signaling plays a key role in brain ultrastructural remodelling in obesity and type 2 diabetes mellitus. *Int. J. Mol. Sci*. 2021;22(11):5427. doi:10.3390/ijms221154.
10. Brennan AM, Mantzoros CS. Drug insight: the role of leptin in human physiology and pathophysiology – emerging clinical applications. *Nat Clin Pract Endocrinol Metab*. 2006;2(6):318–327. doi:10.1038/ncpendmet0196.
11. Bouret S, Levin BE, Ozanne SE. Gene-environment interactions controlling energy and glucose homeostasis and the developmental origins of obesity. *Physiol Rev*. 2015;95(1):47–82. doi:10.1152/physrev.00007.2014.
12. Perry RJ, Resch JM, Douglass AM, et al. Leptin's hunger-suppressing effects are mediated by the hypothalamic-pituitary-adrenocortical axis in rodents. *Proc Natl Acad Sci U S A*. 2019;116(27):13670–13679.doi:10.1073/pnas.1901795116.
13. Zucker LM, Zucker TF. Fatty, a new mutation in the rat. *J Hered*. 1961;52(6):275–278. doi:10.1093/oxfordjournals.jhered.a107093.
14. Johnson PR, Zucker LM, Cruce JAF, et al. Cellularity of adipose depots in the genetically obese Zucker rat. *J Lipid Res*. 1971;12(6):706–7l4. doi:10.1016/S0022-2275(20)39459-1.
15. Bray GA. The Zucker fatty rat: a review. *Fed Proc*. 1977;36:148–153.
16. Johnson PR, Stern JS, Greenwood MRC, et al. Adipose tissue hyperplasia and hyperinsulinemia in Zucker obese female rats: a developmental study. *Metabolism*. Suppl 2. 1978;27(12):1941–1954. doi:10.1016/S0026-0495(78)80011-0.
17. Ogawa Y, Masuzaki H, Isse N, et al. Molecular cloning of rat obese cDNA and augmented gene expression in genetically obese Zucker fatty (fa/fa) rats. *J Clin Invest*. 1995;96(3):1647–1652. doi:10.1172/JCI118204.
18. Iida M, Murakami T, Ishida K, et al. Phenotype-linked amino acid alteration in leptin receptor cDNA from Zucker fatty (fa/fa) rat. *Biochem Biophys Res Commun*. 1996;222(1):19–26. doi:10.1006/bbrc.1996.0691.
19. Iida M, Murakami T, Ishida K, et al. Substitution at codon 269 (Glutamine → Proline) of the leptin receptor (OB-R) cDNA is the only mutation found in the Zucker fatty (fa/fa) rat. *Biochem Biophys Res Commun*. 1996;224(2):597–604. doi:10.1006/bbrc.1996.1070.
20. Takaya K, Ogawa Y, Isse N, et al. Molecular cloning of rat leptin receptor isoform complementary DNAs – identification of a missense mutation in Zucker fatty (fa/fa) rats. *Biochem Biophys Res Commun*. 1996;225 (1):75–83. doi:10.1006/bbrc.1996.1133.
21. Kurtz TW, Morris RC, Pershadsingh HA. The Zucker fatty rat as a genetic model of obesity and hypertension. *Hypertension*. 1989;13(6_pt_2):896–901. doi:10.1161/01.HYP.13.6.896.
22. Beck B, Burlet A, Jean-Pierre Nicolas J-P, et al. Hypothalamic neuropeptide Y (NPY) in obese Zucker rats: implications in feeding and sexual behaviors. *Physiol Behav*. 1990;47(10):449–453. doi:10.1016/0031-9384(90)90107-F.
23. Ahmad I, Steggles AW, Carrillo AJ, et al. Developmental changes in levels of growth hormone mRNA in Zucker rats. *J Cell Biochem*. 1990;43 (1):59–66. doi:10.1002/jcb.240430106.
24. Ahmad I, Finkelstein JA, Downs TR, et al. Obesity-associated decrease in growth hormone-releasing hormone gene expression: a mechanism for reduced growth hormone mRNA levels in genetically obese Zucker rats. *Neuroendocrinology*. 1993;58(3):332–337. doi:10.1159/000126558.
25. Murakami DM, Horwitz BA, Fuller CA. Circadian rhythms of temperature and activity in obese and lean Zucker rats. *Am J Physiol*. 1995;269:R1038–43.
26. Gong D-W, He Y, Karas M, et al. Uncoupling protein-3 Is a mediator of thermogenesis regulated by thyroid hormone, β3-adrenergic agonists, and leptin. *J Biol Chem*. 1997;272(39):24129–24132. doi:10.1074/jbc.272.39.24129.
27. Morton GJ, AEL W, Schwartz MW. Leptin and the central nervous system control of glucose metabolism. *Physiol Rev*. 2011;91(2):389–411. doi:10.1152/physrev.00007.2010.
28. Shi Z, Pelletier NE, Wong J, et al. Leptin increases sympathetic nerve activity via induction of its own receptor in the paraventricular nucleus. *Elife*. 2020;9. doi:10.7554/elife.
29. Gilloteaux J, Jamison E, Finkelstein JA. Calcitonin-cell hyperplasia in obese Zucker rats. *Anat Rec*. 1985;211:69–64A.
30. Gilloteaux J, Pardhan D. Crinophagy in thyroid follicular and parafollicular cells of male obese Zucker rat. *Ultrastruct Pathol*. 2015;39(4):255–269. doi:10.3109/01913123.2015.1014611.
31. Faour O, Gilloteaux J. Calcitonin: survey of new anatomy data to pathology and therapeutic aspects. *Transl Res Anat*. 2017;6:4–15.

32. Gilloteaux J, Solomon N, Subramanian K, et al. The leptin receptor mutation of the obese Zucker rat causes sciatic nerve demyelination with a centripetal pattern defect. *Ultrastruct Pathol*. 2018;42(5):377–408. doi:10.1080/01913123.2018.1522405.
33. Gilloteaux J, Subramanian K, Solomon N, et al. Peripheral nerve demyelination and a leptin receptor mutation: the obese Zucker rat sciatic nerve demyelination occurs with a centripetal pattern defect. *Brain Nerves*. 2019. doi:10.15761/JBN.1000126.
34. Janssen I, Heymsfield SB, Wang Z, et al. Skeletal muscle mass and distribution in 468 men and women aged 18–88 yr. *J Appl Physiol*. 2000;89(1):81–88. doi:10.1152/jappl.2000.89.1.81.
35. Hoppeler H, Luthi P, Claassen H, et al. The ultrastructure of the normal human skeletal muscle: a morphometric analysis on untrained men, women and well-trained orienteers. *Pflugers Arch*. 1973;344(3):217–232. doi:10.1007/BF00588462.
36. He J, Watkins S, Kelley DE. Skeletal muscle lipid content and oxidative enzyme activity in relation to muscle fiber type in type 2 diabetes and obesity. *Diabetes*. 2001;50(4):817. doi:10.2337/diabetes.50.4.817.
37. Tarnopolsky MA, Rennie CD, Robertshaw HA, et al. Influence of endurance exercise training and sex on intramyocellular lipid and mitochondrial ultrastructure, substrate use, and mitochondrial enzyme activity. *Am J Physiol Regul Integr Comp Physiol*. 2007;292(3):R1271–R1278. doi:10.1152/ajpregu.00472.2006.
38. Steinberg GR, Parolin ML, Heigenhauser GJ, et al. Leptin increases FA oxidation in lean but not obese human skeletal muscle: evidence of peripheral leptin resistance. *Am J Physiol Endocrinol Metab*. 2002;283(1):E187–192. doi:10.1152/ajpendo.00542.2001.
39. Larsen S, Stride N, Hey-Mogensen M, et al. Increased mitochondrial substrate sensitivity in skeletal muscle of patients with type 2 diabetes. *Diabetologia*. 2011;54(6):1427–1436. doi:10.1007/s00125-011-2098-4.
40. Lark DS, Fisher-Wellman KH, Neufer PD. High-fat load: mechanism(s) of insulin resistance in skeletal muscle. *Int J Obes Suppl*. 2012;2(Suppl 2):S31–S36. doi:10.1038/ijosup.2012.20.
41. Lowell BB. Mitochondrial dysfunction and type 2 diabetes. *Science*. 2005;307(5708):384–387. doi:10.1126/science.1104343.
42. Patti ME, Corvera S. The role of mitochondria in the pathogenesis of type 2 diabetes. *Endocr Rev*. 2010;31:364–395.
43. Szendroedi J, Phielix E, Roden M. The role of mitochondria in insulin resistance and type 2 diabetes mellitus. *Nat Rev Endocrinol*. 2011;8(2):92–103. doi:10.1038/nrendo.2011.138.
44. Fisher-Wellman KH, Neufer PD. Linking mitochondrial bioenergetics to insulin resistance via redox biology. *Trends Endocrinol Metab*. 2012;23(3):142–153. doi:10.1016/j.tem.2011.12.008.
45. Muoio DM, Neufer PD. Lipid-induced mitochondrial stress and insulin action in muscle. *Cell Metab*. 2012;15(5):595–605. doi:10.1016/j.cmet.2012.04.010.
46. Genders AJ, Holloway GP, Bishop DJ. Are alterations in skeletal muscle mitochondria a cause or consequence of insulin resistance? *Int J Mol Sci*. 2020;22(18):6948. doi:10.3390/ijms21186948. 21.
47. Triolo M, Hoo DA. Manifestations of age on autophagy, mitophagy and lysosomes in skeletal muscle. *Cells*. 2021;10(5):1054. doi:10.3390/cells10051054.
48. Holloszy JO. Skeletal muscle "mitochondrial deficiency" does not mediate insulin resistance. *Am J Clin Nutr*. 2009;89(1):463S–466S. doi:10.3945/ajcn.2008.26717C.
49. Schwerzmann K, Hoppeler H, Kayar SR, et al. Oxidative capacity of muscle and mitochondria: correlation of physiological, biochemical, and morphometric characteristics. *Proc Natl Acad Sci USA;*. 1989;86(5):1583–1587. doi:10.1073/pnas.86.5.1583.
50. Hochachka PW. *Muscles as Molecular and Metabolic Machines*. Boca Raton: FL: CRC; 1994.
51. Toledo FG, Goodpaster BH. The role of weight loss and exercise in correcting skeletal muscle mitochondrial abnormalities in obesity, diabetes and aging. *Mol Cell Endocrinol*. 2013;379(1–2):30–34. doi:10.1016/j.mce.2013.06.018.
52. Lebon V, Dufour S, Petersen KF, et al. Effect of triiodothyronine on mitochondrial energy coupling in human skeletal muscle. *J Clin Invest*. 2001;108(5):733–737. doi:10.1172/JCI200111775.
53. Anderson EJ, Lustig ME, Boyle KE, et al. Mitochondrial H_2O_2 emission and cellular redox state link excess fat intake to insulin resistance in both rodents and humans. *J Clin Invest*. 2009;119(3):573–581. doi:10.1172/JCI37048.
54. Galicia-Garcia U, Benito-Vicente A, Jebari S, et al. Pathophysiology of type 2 diabetes mellitus. *Int J Mol Sci*. 2020;21(17):6275.doi:10.3390/ijms21176275.
55. Beeson M, Sajan MP, Dizon M, et al. Activation of protein kinase C-zeta by insulin and phosphatidylinositol-3,4,5-(PO4)3 is defective in muscle in type 2 diabetes and impaired glucose tolerance: amelioration by rosiglitazone and exercise. *Diabetes*. 2003;52(8):1926–1234. doi:10.2337/diabetes.52.8.1926.
56. Kuhlmann J, Neumann-Haefelin C, Belz U, et al. Intramyocellular lipid and insulin resistance: a longitudinal in vivo ^{1}H-spectroscopic study in Zucker diabetic fatty rats. *Diabetes*. 2003;52(1):138–144. doi:10.2337/diabetes.52.1.138.

57. Gilloteaux J, Bissler J. Morphological aspects of the obese Zucker rat skeletal muscle tissue. *J Cell Biol*. 1984;99:437–437a.
58. Gilloteaux J, Bissler J, Payne W, et al. Histo-enzymatic changes induced by exercise in Zucker rat skeletal muscles. *Am Zool*. 1985;25(40):A121.
59. Chavez JA, Knotts TA, Wang LP, et al. A role for ceramide, but not diacylglycerol, in the antagonism of insulin signal transduction by saturated fatty acids. *J Biol Chem*. 2003;278(12):10297–10303. doi:10.1074/jbc.M212307200.
60. Savage DB, Petersen KF, Shulman GI. Disordered lipid metabolism and the pathogenesis of insulin resistance. *Physiol Rev*. 2007;87(2):507–520. doi:10.1152/physrev.00024.2006.
61. Boini KM, Xia M, Koka S, et al. Sphingolipids in obesity and related complications. *Front Biosci (Landmark Ed)*. 2017;22(1):96–116. doi:10.2741/4474.
62. Chavez JA, Summers SA. A ceramide-centric view of insulin resistance. *Cell Metab*. 2012;15(5):585–594. doi:10.1016/j.cmet.2012.04.002.
63. Mandal N, Grambergs R, Mondal K, et al. Role of ceramides in the pathogenesis of diabetes mellitus and its complications. *J Diabetes Compl*. 2021;35:107734. doi:10.1016/j.jdiacomp.2020.107734.
64. Doblado L, Lueck C, Rey C, et al. Mitophagy in human diseases. *Int J Mol Sci*. 2021;22(8):3903.doi:10.3390/ijms22083903.
65. Katzberg H, Kokokyi S, Halpern E, et al. Prevalence of muscle cramps in patients with diabetes. *Diabetes*. 2014;37(1):e17–e18.doi:10.2337/dc13-1163.
66. Payne W, Lemon P, Bissler J, et al., R7 abstract. Role of endurance exercise in inducing left ventricular hypertrophy in the genetically obese Zucker rat. *J Mol Cell Cardiol*. 1985;17:vii–vii. doi:10.1016/S0022-2828(85)80357-6.
67. Paradise NF, Pilati CF, Payne WR, et al. Left ventricular function of the isolated genetically obese rat's heart. *Am J Physiol*. 1985;248:H438–444.
68. Guth L, Samaha FJ. Qualitative differences between actomyosin ATPase of slow and fast mammalian muscle. *Exp Neurol*. 1969;25(1):138–152. doi:10.1016/0014-4886(69)90077-6.
69. Nachlas MM, Tsou K, DeSouza E, et al. Cytochemical demonstration of succinic dehydrogenase by the use of a new *p*-nitrophenyl substituted ditetrazole. *J Histochem Cytochem*. 1957;5(4):420–436. doi:10.1177/5.4.420.
70. Gilloteaux J, Ader M. Histochemical demonstration of AMP deaminase activity in hamster skeletal muscle tissues. *Acta Histochem*. 1984;73(1):47–51. doi:10.1016/S0065-1281(83)80074-9.
71. Yarasheski KE, Lemon PWR, Gilloteaux J. Effect of heavy resistance exercise training on young rat muscle fiber composition. *J Appl Physiol*. 1990;69(2):434–437. doi:10.1152/jappl.1990.69.2.434.
72. Aroniadou-Andrejaska V, Lemon PWR, Gilloteaux J. Effects of exogenous growth hormone on skeletal muscle of young female rats. *Tissue Cell*. 1996;28(6):719–724. doi:10.1016/S0040-8166(96)80074-7.
73. Song SK, Shimada N, Anderson PJ. Orthogonal diameters in the analysis of muscle fiber size and form. *Nature London*. 1963;200(4912):1220–1221. doi:10.1038/2001220a0.
74. Bortoff A, Gilloteaux J. Specific tissue impedances of estrogen- and progesterone-treated rabbit myometrium. *Am J Physiol*. 1980;238(7):C34–42. doi:10.1152/ajpcell.1980.238.1.C34.
75. Gilloteaux J, Szczepanski M. The fibre dimensions of uterine smooth muscle of the rabbit following treatment by female sex steroids. *Tissue Cell*. 2000;32(3):243–248. doi:10.1054/tice.2000.0112.
76. Karnovsky MJ. The ultrastructural basis of capillary permeability studied with peroxidase as a tracer. *J Cell Biol*. 1967;35(1):213–236. doi:10.1083/jcb.35.1.213.
77. Hanson J, Huxley JE. The structural bases of contraction in striated muscle. *Symp Soc Exp Biol*. 1955;9:228–264.
78. Huxley AF. Muscle structure and theories of contraction. *Prog Biophys Chem*. 1957;7:258–318.
79. Needham DM. *Machina Carnis. The Biochemistry of Muscular Contraction in Its Historical Development*. Cambridge: Cambridge University Press; 1971.
80. Schmalbruch H. *Skeletal Muscles*. Berlin and Heidelberg: Springer Verlag; 1985. XII+1-440.
81. Kellermayer MSZ. *Muscle Contraction: A Hungarian Perspective*. Budapest: Semmelweiss Publishers; 2018: ISBN-13: 978-9633314562.
82. Rosa C, Tsou K-C. Use of tetrazolium compounds in oxidative enzyme histo- and cyto- chemistry. *Nature*. 1961;192(4806):990–991. doi:10.1038/192990a0.
83. Dubowitz V, Brooke MH, Neville HE. *Muscle Biopsy: A Modern Approach*. London: WB Saunders Co Ltd; 1973:138–143.
84. Ambrustmacher VW. Skeletal muscle. In: *JB Lippincott Pathology*. Rubin E, Farber J, eds., 2d. Philadelphia: JB Lippincott;1994:1349-1370
85. Pette D, Staron RS. Mammalian skeletal muscle fiber type transitions. *Int Rev Cytol*. 1997;170:143–223.
86. Hilber K, Galler S, Gohlsch B, et al. Kinetic properties of myosin chain isoforms in single fibers from human skeletal muscle. *FEBS Lett*. 1999;455(3):267–270. doi:10.1016/S0014-5793(99)00903-5.
87. Pette D, Peuker H, Staron RS. The impact of biochemical methods for single muscle fibre analysis. *Acta Physiol Scand*. 1999;166(4):261–277. doi:10.1046/j.1365-201x.1999.00573.x.
88. Scott W, Stevens J, Binder-Macleod SA. Human skeletal muscle fiber type classifications. *Phys Ther*. 2001;81(11):1810–1816. doi:10.1093/ptj/81.11.1810.

89. Schiaffino S, Reggiani C. Fiber types in mammalian skeletal muscles. *Physiol Rev*. 2011;91(4):1447–1531. doi:10.1152/physrev.00031.2010.
90. Wu P, Zhang S, Spinner RJ, et al. A novel triple immunoenzyme staining enables simultaneous identification of all muscle fiber types on a single skeletal muscle cryosection from normal, denervated or reinnervated rats. *Neural Regen Res*. 2017;12(8):1357–1364. doi:10.4103/1673-5374.213560.
91. Dubowitz V, Sewry CA, Oldfors A. *Muscle Biopsy. A Practical Approach*. 5th. Amsterdam: Elsevier. ISBN 978-0-7020-7471-4; 2020.
92. Peter JB, Barnard RT, Edgerton VR, et al. Metabolic profiles of three fiber types of skeletal muscle in Guinea pigs and rabbits. *Biochemistry*. 1972;11 (14):2627–2633. doi:10.1021/bi00764a013.
93. Muntener M. Variable pH dependence of the myosin ATPase in different muscles of the rat. *Histochemistry*. 1979;62(3):299–304. doi:10.1007/BF00508358.
94. Armstrong RB, Phelps RO. Muscle fiber type composition of the rat hindlimb. *Am J Anat*. 1984;171 (3):259–272. doi:10.1002/aja.1001710303.
95. Ariano MA, Armstrong RB, Edgerton VR. Hindlimb muscle fiber populations of five mammals. *J Histochem Cytochem*. 1973;21(1):51–55. doi:10.1177/21.1.51.
96. Fisher ER, Danowski TS. Electron microscopy in the study of disorders of skeletal muscle. *Pathol Annu*. 1974;9:345–384.
97. Jerusalem F, Engel AG, Peterson HA. Human muscle fiber fine structure: morphometric data on controls. *Neurology*. 1975;25(2):127–134. doi:10.1212/wnl.25.2.127.
98. MacIntosh BR, Gardiner PF, McComas AJ. *Skeletal Muscle: Form and Function*. 2nd. Champaign, Ill.: Human Kinetics; 2006.
99. Campion DR, Shapira JF, Allen CE, et al. Metabolic characteristics of skeletal muscle from lean and obese Zucker rats. *Growth*. 1987;51(4):397–410.
100. Pénicaud L, Ferré P, Terretaz J, et al. Development of obesity in Zucker rats. Early insulin resistance in muscles but normal sensitivity in white adipose tissue. *Diabetes*. 1987;36(5):626–631. doi:10.2337/diab.36.5.626.
101. Pénicaud DL, Picon L, Picon L. Résistance à l'insuline des muscles chez le rat Zucker lors de l'installation de l'obésité. *Reprod Nutr Dévelop*. 1988;28(3B):823–824. French. doi:10.1051/rnd:19880519.
102. Acevedo LM, Raya AI, Ríos R, et al. Obesity-induced discrepancy between contractile and metabolic phenotypes in slow- and fast-twitch skeletal muscles of female obese Zucker rats. *J Appl Physiol*. 2017;123(1):249–259. doi:10.1152/japplphysiol.00282.2017.
103. Tasić D, Dimov D, Gligorijević J, et al. Muscle fibre types and fibre morphometry in the tibialis posterior and anterior of the rat: a comparative study. *Facta Universitatis*. 2003;10(1):16–21.
104. Tasić D, Dimov I, Petrović V, et al. Fiber type composition and size of fibers in the rat tibialis anterior muscle. *Sci J Fac Med Niš*. 2011;28(3):161–168.
105. Melo RTR, Damázio LCM, Lima MC, et al. Effects of physical exercise on skeletal muscles of rats with cerebral ischemia. *Braz J Med Biol Res*. 2019;52(12):e8576. doi:10.1590/1414-431X2019857.
106. Termin A, Staron RS, Pette D. Myosin heavy chain isoforms in histochemically defined fiber types of rat muscle. *Histochemistry*. 1989;92(6):453–457. doi:10.1007/BF00524756.
107. Pullen AH. The distribution and relative sizes of three histochemical fibre types in the rat tibialis anterior muscle. *J Anat*. 1977;123:1–19.
108. Torrella JR, Whitmore JM, Casas M, et al. Capillarity, fibre types and fibre morphometry in different sampling sites across and along the tibialis anterior muscle of the rat. *Cells Tissues Organs*. 2000;167(2–3):153–162. doi:10.1159/000016778.
109. Wang LC, Kernell D. Fibre type regionalization in lower hindlimb muscles of rabbit, rat and mouse: a comparative study. *J Anat*. 2001;199(6):631–643. doi:10.1046/j.1469-7580.2001.19960631.x.
110. Cornachione A, Cacao-Benedini LO, Shimano MM, et al. Morphological comparison of different protocols of skeletal muscle remobilization in rats after hindlimb suspension. *Scand J Med Sci Sports*. 2008;18(4):453–461. doi:10.1111/j.1600-0838.2007.00720.x.
111. De Koning JJ, van der Molen HF, Woittiez RD, et al. Functional characteristics of rat gastrocnemius and tibialis anterior muscles during growth. *J Morphol*. 1987;194(1):75–84. doi:10.1002/jmor.1051940107.
112. Haggarty P, Reeds PJ, Fletcher JM, et al. The fate of ^{14}C derived from radioactively labelled dietary precursors in young rats of the Zucker strain (Fa/- and fa/fa). *Biochem J*. 1986;235(2):323–327. doi:10.1042/bj2350323.
113. Durschlag RP, Layman DK. Skeletal muscle growth in lean and obese Zucker rats. *Growth*. 1983;47:282–291.
114. Wool IG. Effects of insulin on cellular protein synthesis. In: Insulin by. Hasselblatt A, and Bruchhausen FV, eds. Vol. 2. Berlin: Springer-Verlag; 1975:268–302.
115. Katta A, Karkala SK, Wu M, et al. Lean and obese Zucker rats exhibit different patterns of p70s6 kinase regulation in the tibialis anterior muscle in response to high-force muscle contraction. *Muscle Nerve*. 2009;39 (4):503–511. doi:10.1002/mus.21255.
116. Azain MJ, Broderson JR, Martin RJ. Effect of long-term somatotropin treatment on body composition and life span in aging obese Zucker rats. *Exp Biol Med (Maywood)*. 2006;231(1):76–83. doi:10.1177/153537020623100109.
117. Shapira JF, Kircher I, Martin AJ. Indices of skeletal muscle growth in lean and obese Zucker rats. *J Nutr*. 1980;110(7):1313–1318. doi:10.1093/jn/110.7.1313.

118. Wallis MG, Wheatley CM, Rattigan S, et al. Insulin-mediated hemodynamic changes are impaired in muscle of Zucker obese rats. *Diabetes*. 2002;51(12):3492–3498. doi:10.2337/diabetes.51.12.3492.
119. Goossens GH, Jocken JWE, Blaak EE. Sexual dimorphism in cardiometabolic health: the role of adipose tissue, muscle and liver. *Nat Rev Endocrinol*. 2021;17:47–66.
120. Mullur R, Liu YY, Brent GA. Thyroid hormone regulation of metabolism. *Physiol Rev*. 2014;94(2):355–382. doi:10.1152/physrev.00030.2013.
121. Frisbee JC, Delp MD. Vascular function in the metabolic syndrome and the effects on skeletal muscle perfusion: lessons from the obese Zucker rat. *Essays Biochem*. 2006;42:145–161. doi:10.1042/bse0420145.
122. Ghosh D, Peng J, Brown K, et al. Super-resolution ultrasound imaging of skeletal muscle microvascular dysfunction in an animal model of type 2 diabetes. *J Ultrasound Med*. 2019;38(10):2589–2599. doi:10.1002/jum.14956.
123. Prior SJ, Blumenthal JB, Katzel LI, et al. Increased skeletal muscle capillarization after aerobic exercise training and weight loss improves insulin sensitivity in adults with IGT. *Diabetes Care*. 2014;37(5):1469–1475. doi:10.2337/dc13-2358.
124. Perry BD, Caldow MK, Brennan-Speranza TC, et al. Muscle atrophy in patients with type 2 diabetes mellitus: roles of inflammatory pathways, physical activity and exercise. *Exerc Immunol Rev*. 2016;22:94–109.
125. Srikanthan P, Hevener AL, Karlamangla AS. Sarcopenia exacerbates obesity-associated insulin resistance and dysglycemia: findings from the National Health and Nutrition Examination Survey III. *PLoS One*. 2010;5(5):e10805. doi:10.1371/journal.pone.0010805.
126. Hoppeler H. Exercise-induced ultrastructural changes in skeletal muscle. *Int J Sports Med*. 1986;7(4):187–204. doi:10.1055/s-2008-1025758.
127. Kelley DE, Simoneau J-A. Impaired FFA utilization by skeletal muscle in NIDDM. *J Clin Invest*. 1994;94(6):2349–2356. doi:10.1172/JCI117600.
128. Chomentowski P, Coen PM, Radiková Z, et al. Skeletal muscle mitochondria in insulin resistance: differences in intermyofibrillar versus subsarcolemmal subpopulations and relationship to metabolic flexibility. *J Clin Endocrinol Metab*. 2011;96(2):494–503. doi:10.1210/jc.2010-0822.
129. Kelley DE, He J, Menshikova EV, et al. Dysfunction of mitochondria in human skeletal muscle in type 2 diabetes. *Diabetes*. 2002;51(10):2944–2950. doi:10.2337/diabetes.51.10.2944.
130. Mastaglia FL, Sir WJ. *Skeletal Muscle Pathology*. Edinburgh: Churchill Livingstone; 1982:404–408.
131. Carpenter S, Karpati G. *Pathology of Skeletal Muscle*. 2nd. New York: Oxford University Press; 2001.
132. Malfatti E, Romero NB. Chapter 30 - Diseases of the skeletal muscle. *Handb Clin Neurol*. 2018;145:429–451.
133. Ohkuma A, Noguchi S, Sugie H, et al. Clinical and genetic analysis of lipid storage myopathies. *Muscle Nerve*. 2009;39(3):333–342. doi:10.1002/mus.21167.
134. Angelini C, Federico A, and Reichmann H, et al. Fatty acid mitochondrial disorders. In: *European Handbook of Neurological Management*. Vol. 1. Gilhus NE, Barnes MP, and Brainin M, eds. 2nd. Blackwell Publishing Ltd. 2010;37:923–929. ISBN: 9781405185332.
135. Couser N, Gucsavas-Calikoglu M. Mitochondrial disorders in biomarkers in inborn errors of metabolism. *Clin Aspects Lab Determination*. 2017;167–190. [Chapter 8]. doi:10.1016/B978-0-12-802896-4.00008-0.
136. De Feyter HM, Schaart G, Hesselink MK, et al. Regional variations in intramyocellular lipid concentration correlate with muscle fiber type distribution in rat tibialis anterior muscle. *Magn Reson Med*. 2006;56(1):19–25. doi:10.1002/mrm.20924.
137. Shulman GI, Rothman D, Jue T, et al. Quantitation of muscle glycogen synthesis in normal subjects and subjects with non-insulin-dependent diabetes by ^{13}C nuclear magnetic resonance spectroscopy. *N Engl J Med*. 1990;322(4):223–228. doi:10.1056/NEJM199001253220403.
138. Taylor R, Price TB, Rothman DL, et al. Validation of^{13}c nmr measurement of human skeletal muscle glycogen by direct biochemical assay of needle biopsy samples. *Magn Reson Med*. 1992;27(1):13–20. doi:10.1002/mrm.1910270103.
139. Reeves ND, Maganaris CN, Narici MV. Ultrasonographic assessment of human skeletal muscle size. *Eur J Appl Physiol*. 2004;91(1):116–118. doi:10.1007/s00421-003-0961-9.
140. Tahallah N, Brunelle A, De La Porte S, et al. Lipid mapping in human dystrophic muscle by cluster-time-of-flight secondary ion mass spectrometry imaging. *J Lipid Res*. 2008;49(2):438–454. doi:10.1194/jlr.M700421-JLR200.
141. Honka M-J, Latva-Rasku A, Bucci M, et al. Insulin-stimulated glucose uptake in skeletal muscle, adipose tissue and liver: a positron emission tomography study. *Eur J Endocrinol*. 2018;178(5):523–531. doi:10.1530/EJE-17-0882.
142. Rudroff T, Ketelhut NB, Kindred JH. Metabolic imaging in exercise physiology. *J Appl Physiol*. 2018;124(2):497–503. doi:10.1152/japplphysiol.00898.2016.
143. Lally JSV, Snook LA, Han XX, et al. Subcellular lipid droplet distribution in red and white muscles in the obese Zucker rat. *Diabetologia*. 2012;55(2):479–488. doi:10.1007/s00125-011-2367-2.
144. Ginjupalli GK, Rice KM, Katta A, et al. High-frequency electrical stimulation (HFES) data lean and obese Zucker rat tibialis anterior muscle: regulation of glycogen synthase kinase 3 beta (GSK3B) associated proteins. *Data Brief*. 2017;16:423–429. doi:10.1016/j.dib.2017.11.036.

145. Fujii T, Ishikawa S, Uga S. Ultrastructure of iris muscles in diabetes mellitus. *Ophthalmologica*. 1977;174 (4):228–239. doi:10.1159/000308607.
146. Ishikawa S, Bensaoula T, Uga S, et al. Electron-microscopic study of iris nerves and muscles in diabetes. *Ophthalmologica*. 1985;191(3):172–183. doi:10.1159/000309582.
147. Fujimoto Y, Ohsaki Y, Cheng J, et al. Lipid droplets: a classic organelle with new outfits. *Histochem Cell Biol*. 2008;130(2):263–279. doi:10.1007/s00418-008-0449-0.
148. Ghadially FN. *Ultrastructural Pathology of the Cell and Matrix*. Vol. 1. 2nd. Boston: Butterworth-Heinemann; 1997:252–254. 2: 1035-1037.
149. Walther TC, Farese RV Jr. Lipid droplets and cellular lipid metabolism. *Annual Review of Biochemistry*. 2012;81(1):687–714. doi:10.1146/annurev-biochem-061009-102430.
150. van der Vusse GJ, Reneman RS. Lipid metabolism in muscle. In: Compreghensive Physiology, R. Terjung (Ed). *Handbook of Physiology, Exercise: Regulation and Integration of Multiple Systems*. 2011; 952-994. doi:10.1002/cphy.cp120121
151. Stein O, Stein Y. Lipid synthesis, intracellular transport, and secretion. II. Electron microscopic radioautographic study of the mouse lactating mammary gland. *J Cell Biol*. 1967;34(1):251–263. doi:10.1083/jcb.34.1.251.
152. Blanchette-Mackie EJ, Dwyer NK, Barber T, et al. Perilipin is located on the surface layer of intracellular lipid droplets in adipocytes. *J Lipid Res*. 1995;36 (6):1211–1226. doi:10.1016/S0022-2275(20)41129-0.
153. Benador IY, Veliova M, Mahdaviani K, et al. Mitochondria bound to lipid droplets have unique bioenergetics, composition, and dynamics that support lipid droplet expansion. *Cell Metab*. 2018;27(4):869–885. doi:10.1016/j.cmet.2018.03.003.
154. Seibert JT, Najt CP, Heden TD, et al. Muscle lipid droplets: cellular signaling to exercise physiology and beyond. *Trends Endocrinol Metab*. 2020;1534. doi:10.1016/j.tem.2020.08.002.
155. Saini-Chohan HK, Mitchell RW, Vaz FM, et al. Delineating the role of alterations in lipid metabolism to the pathogenesis of inherited skeletal and cardiac muscle disorders: thematic review series: genetics of human lipid diseases. *J Lipid Res*. 2012;53(1):4–27.
156. van Loon LJ, Koopman R, Manders R, et al. Intramyocellular lipid content in type 2 diabetes patients compared with overweight sedentary men and highly trained endurance athletes. *Am J Physiol Endocrinol Metab*. 2004;287(3):E558–65. doi:10.1152/ajpendo.00464.2003.
157. Devries MC, Samjoo IA, Hamadeh MJ, et al. Endurance training modulates intramyocellular lipid compartmentalization and morphology in skeletal muscle of lean and obese women. *J Clin Endocrinol Metab*. 2013;98 (12):4852–4862. doi:10.1210/jc.2013-2044.
158. Pernow B, Saltin B. *Muscle Metabolism during Exercise*. New York-London: Plenum Press; 1971.
159. Gilloteaux J. Ultrastructural aspects of atrium development: demonstration of endocardial discontinuities and immunolabeling of atrial natriuretic factor in the Syrian hamster. *Anat Embryol*. 1989;179(3):227–236. doi:10.1007/BF00326587.
160. Gilloteaux J, Linz D. Endocardial surface and atrial morphological changes in fetal, neonatal, and old adult Syrian hamster. *Am J Anat*. 1989;186(2):161–172. doi:10.1002/aja.1001860206.
161. Gilloteaux J, and Linz D. Endocardial surface changes during atrium development. A TEM, SEM and ANF immunolabeling. New York Acad Sci. In: *Embryonic Origins of Defective Heart Development*. Vol. 588 J Wiley (New york). 1990;373–376.
162. Gilloteaux J, Naud J. The zinc iodide-osmium tetroxide staining-fixative of Maillet: microanalysis and detection of Ca2+-affinity subcellular sites in a smooth muscle. *Histochemistry*. 1979;63(2):227–243. doi:10.1007/BF00644545.
163. Belazi D, Solé-Domènech S, Johansson B, et al. Chemical analysis of osmium tetroxide staining in adipose tissue using imaging ToF-SIMS. *Histochem Cell Biol*. 2009;132(1):105–115. doi:10.1007/s00418-009-0587-z.
164. Ericsson JLE, Saladino J, Trump F. Electron microscopic observations of the influence of different fixatives on the appearance of cellular ultrastructure. *Z Zellforsch*. 1965;66(2):161–181. doi:10.1007/BF00344332.
165. Wood L, Luft JH. The influence of buffer systems on fixation with osmium tetroxide. *J Ultrastruct Res*. 1965;12(1–2):22–45. doi:10.1016/S0022-5320(65)80004-1.
166. Angermüller S, Fahimi HD. Imidazole-buffered osmium tetroxide: an excellent stain for visualization of lipids in transmission electron microscopy. *Histochem J*. 2005;14 (5):823–835. doi:10.1007/BF01033631.
167. Randle PJ, Garland PB, Hales CN, Newsholme EA. The glucose fatty-acid cycle. Its role in insulin sensitivity and the metabolic disturbances of diabetes mellitus. *Lancet*. 1963;1(7285):785–789. doi:10.1016/S0140-6736(63)91500-9.
168. Boden G. Role of fatty acids in the pathogenesis of insulin resistance and NIDDM. *Diabetes*. 1997;46 (1):3–10. doi:10.2337/diab.46.1.3.
169. Brechtel K, Machann J, Jacob S, et al. In vivo 1H-MR spectroscopy: determination of the intra- and extramyocellular lipid contents in dependence on insulin action in young offspring of type 2 diabetic subjects. *Fortschr Roentgenstr*. 1999;171:113–120.
170. Boesch C, Kreis R. Observation of intramyocellular lipids by ^{1}H-magnetic resonance spectroscopy. *Ann N Y Acad Sci*. 2000;904(1):25–31. doi:10.1111/j.1749-6632.2000.tb06417.x.

171. Goodpaster BH, He J, Watkins S, et al. Skeletal muscle lipid content and insulin resistance: evidence for a paradox in endurance-trained athletes. *J Clin Endocrinol & Metab*. 2001;86(12):5755–5761. doi:10.1210/jcem.86.12.8075.
172. Dubé JJ, Amati F, Stefanovic-Racic M, et al. Exercise-induced alterations in intramyocellular lipids and insulin resistance: the athlete's paradox revisited. *Am J Physiol Endocrinol Metab*. E882-E888. 2008;294(5): E882–E888. doi:10.1152/ajpendo.00769.2007.
173. Franklin RM, Kanaley JA. Intramyocellular lipids: effect of age, obesity, and exercise. *Phys Sportsmed*. 2009;37 (1):20–26. doi:10.3810/PSM.2009.04.1679.
174. Samuel VT, Petersen KF, Shulman GI. Lipid-induced insulin resistance: unravelling the mechanism. *Lancet*. 2010;375(9733):2267–2277. doi:10.1016/S0140-6736(10)60408-4.
175. Debashree B, Kumar M, Subrahmanya T, et al., Mitochondrial dysfunction in human skeletal muscle biopsies of lipid storage disorder. *J Neurochem*. 2018; 145(4): 323–341. 10.1111/jnc.14318
176. Boyle KE, Canham JP, Consitt LA, et al. A high-fat diet elicits differential responses in genes coordinating oxidative metabolism in skeletal muscle of lean and obese individuals. *J Clin Endocrinol Metab*. 2011;96 (3):775–781. doi:10.1210/jc.2010-2253.
177. Shah K, Villareal DT. Weight loss and improved fitness slow down the decline in mobility in obese adults with type 2 diabetes. *Evidence-Based Med*. 2013;18(2):e18–e18. 10.1136/eb-2012-100788 in ebmed.18.2. e 18. doi:10.1136/eb-2012-100788.
178. Schmitt B, Flück M, Décombaz J, et al. Transcriptional adaptations of lipid metabolism in tibialis anterior muscle of endurance-trained athletes. *Physiol Genomics*. 2003;15 (2):148–157. doi:10.1152/physiolgenomics.00089.2003.
179. Colberg SR, Simoneau J-A, Thaete FL, et al. Impaired FFA utilization by skeletal muscle in women with visceral obesity. *J Clin Invest*. 1995;95(4):1846–1853. doi:10.1172/JCI117864.
180. Kahn D, Perreault L, Macias E, et al. Subcellular localisation and composition of intramuscular triacylglycerol influence insulin sensitivity in humans. *Diabetologia*. 2021;64(1):168–180. doi:10.1007/s00125-020-05315-0.
181. Gemmink A, Daemen S, Brouwers B, et al. Dissociation of intramyocellular lipid storage and insulin resistance in trained athletes and type 2 diabetes patients; involvement of perilipin 5?. *J Physiol*. 2018;596(5):857–868. doi:10.1113/JP275182.
182. Ryan AS, Ortmeyer HK. Obesity and insulin resistance, metabolic flexibility and insulin suppression of skeletal muscle LPL activity increase with AEX + WL in overweight and obese, sedentary older women. *Int J Obesity*. 2019;43(2):276–284. doi:10.1038/s41366-018-0068-3.
183. Colleluori G, Aguirre L, Phadnis U, et al. Aerobic plus resistance exercise in obese older adults improve muscle protein synthesis and preserves myocellular quality despite weight loss. *Cell Metab*. 2019;30(2):261–273.e6. doi:10.1016/j.cmet.2019.06.008.
184. Blaak EE, Wagenmakers AJM, Glatz JFC, et al. Plasma FFA utilization and fatty acid-binding protein content are diminished in type 2 diabetic muscle. *Am J Physiol*. 2000;279:146–154.
185. Tunstall RJ, Mehan KA, Wadley GD, et al. Exercise training increases lipid metabolism gene expression in human skeletal muscle. *Am J Physiol Endocrinol Metab*. 2002;283(1):E66–E72. doi:10.1152/ajpendo.00475.2001.
186. Patti ME, Butte AJ, Crunkhorn S, et al. Coordinated reduction of genes of oxidative metabolism in humans with insulin resistance and diabetes: potential role of PGC1 and NRF1. *Proc Natl Acad Sci USA*. 2003;100 (14):8466–8471. doi:10.1073/pnas.1032913100.
187. Mootha VK, Lindgren CM, Eriksson KF, et al. PGC-1alpha-responsive genes involved in oxidative phosphorylation is co-ordinately downregulated in human diabetes. *Nat Genet*. 2003;34(3):267–273. doi:10.1038/ng1180.
188. Muoio DM. Intramuscular triacylglycerol and insulin resistance: guilty as charged or wrongly accused? *Biochim Biophys Acta*. 2010;1801(3):281–288. doi:10.1016/j.bbalip.2009.11.007.
189. Schrauwen-Hinderling VB, Hesselink MK, Schrauwen P, et al. Intramyocellular lipid content in human skeletal muscle. *Obesity (Silver Spring)*. 2006;14 (3):357–367. doi:10.1038/oby.2006.47.
190. Kakehi S, Tamura Y, Takeno K, et al. Endurance runners with intramyocellular lipid accumulation and high insulin sensitivity have enhanced expression of genes related to lipid metabolism in muscle. *J Clin Med*. 2020;9(12):3951.doi:10.3390/jcm9123951.
191. Gollnick PD, King DW. Effect of exercise and training on mitochondria of rat skeletal muscle. *Amer J Physiol*. 1969;216(6):1502–1509. doi:10.1152/ajplegacy.1969.216.6.1502.
192. Ezaki O, Higuchi M, Nakatsuka H, et al. Exercise training increases glucose transporter content in skeletal muscles more efficiently from aged obese rats than young lean rats. *Diabetes*. 1992;41(8):920–926. doi:10.2337/diab.41.8.920.
193. Luiken JJ, Arumugam Y, Dyck DJ, et al. Increased rates of fatty acid uptake and plasmalemmal fatty acid transporters in obese Zucker rats. *J Biol Chem*. 2001;276 (44):40567–40573. doi:10.1074/jbc.M100052200.
194. Kühlmann J, Neumann-Haefelin C, Belz U, et al., Intramyocellular lipid and insulin resistance: a longitudinal in vivo ^{1}H-spectroscopic study in Zucker diabetic fatty rats. *Diabetes*. 2003; 52(1): 138–144. 10.2337/diabetes.52.1.138

195. Korach-André M, Gounarides J, Deacon R, et al. Age and muscle-type modulated role of intramyocellular lipids in the progression of insulin resistance in non-diabetic Zucker rats. *Metabolism*. 2005;54(4):522–528. doi:10.1016/j.metabol.2004.11.006.
196. Shepherd SO, Cocks M, Tipton KD, et al. Sprint interval and traditional endurance training increase net intramuscular triglyceride breakdown and expression of perilipin 2 and 5. *J Physiol*. 2013;591(3):657–675. doi:10.1113/jphysiol.2012.240952.
197. Koh HE, Ørtenblad N, Winding KM, et al. High-intensity interval, but not endurance, training induces muscle fiber type-specific subsarcolemmal lipid droplet size reduction in type 2 diabetic patients. *Am J Physiol Endocrinol Metab*. Nov 1 2018;315(5):E872–E884. doi:10.1152/ajpendo.00161.2018.
198. Holloway GP, Benton C, Mullen KL, et al. In obese rat muscle transport of palmitate is increased and is channelled to triacylglycerol storage despite an increase in mitochondrial palmitate oxidation. *Am J Physiol Endocrinol Metab*. 2009;296(4):E738–E747. doi:10.1152/ajpendo.90896.2008.
199. Kristensen D, Prats C, Larsen S, Ara I, Dela F, Helge JW. Ceramide content is higher in type I compared to type II fibers in obesity and type 2 diabetes mellitus. *Acta Diabetol*. 2013;50(5):705–712. doi:10.1007/s00592-012-0379-0.
200. Fillmore N, Keung W, Kelly SE, et al. Accumulation of ceramide in slow-twitch muscle contributes to the development of insulin resistance in the obese JCR: LA-cp rat. *Exp Physiol*. 2015;100(6):730–741. doi:10.1113/EP085052.
201. Senkal CE, Salama MF, Snider AJ, et al. Ceramide is metabolized to acylceramide and stored in lipid droplets. *Cell Metab*. 2017;25(3):686–697. doi:10.1016/j.cmet.2017.02.010.
202. Broskey NT, Obanda DN, Burton JH, et al. Skeletal muscle ceramides and daily fat oxidation in obesity and diabetes. *Metabolism*. 2018;82:118–123. doi:10.1016/j.metabol.2017.12.012.
203. Sokolowska E, Blachnio-Zabielska A. The role of ceramides in insulin resistance. *Front Endocrinol (Lausanne)*. 2019;10:577. doi:10.3389/fendo.2019.00577.
204. Turpin-Nolan SM, Bruning JC. The role of ceramides in metabolic disorders: when size and localization matters. *Nat Rev Endocrinol*. 2020;16(4):224–233. doi:10.1038/s41574-020-0320-5.
205. Kjellberg MA, Lönnfors M, Slotte JP, et al. Metabolic conversion of ceramides in HeLa cells - A cholesteryl phosphocholine delivery approach. *PLoS One*. 2015;10(11):e0143385. doi:10.1371/journal.pone.0143385.
206. Megha E. London, Ceramide selectively displaces cholesterol form ordered lipid domains (rafts): implications for lipid raft structure and function. *J Biol Chem*. 2004;279(11):9997–10004. doi:10.1074/jbc.M309992200.
207. Haus JM, Kashyap SR, Kasumov T, et al. Plasma ceramides are elevated in obese subjects with type 2 diabetes and correlate with the severity of insulin resistance. *Diabetes*. 2009;58(2):337–343. doi:10.2337/db08-1228.
208. Sot J, Goñi FM, Alonso A. Molecular associations and surface-active properties of short-and long-N-acyl chain ceramides. *Biochim Biophys Acta*. 2005;1711(1):12–19. doi:10.1016/j.bbamem.2005.02.014.
209. Arumugam S, Schmieder S, Pezeshkian W, et al. Ceramide structure dictates glycosphingolipid nanodomain assembly and function. *Nature Comm*. 2021;12(1):3675.doi:10.1038/s41467-021-23961-9.
210. Anishkin A, Sukharev S, Colombini M. Searching for the molecular arrangement of transmembrane ceramide channels. *Biophys J*. 2006;90(7):2414–2426. doi:10.1529/biophysj.105.071977.
211. Galadari S, Rahman A, Pallichankandy S, et al. Role of ceramide in diabetes mellitus: evidence and mechanisms. *Lipids Health Dis*. 2013;12(1):98: 1–16. http://www.lipidworld.com/content/12/1/98 .
212. Mogensen M, Sahlin K, Fernström M, et al. Mitochondrial respiration is decreased in skeletal muscle of patients with type 2 diabetes. *Diabetes*. 2007;56(6):1592–1599. doi:10.2337/db06-0981.
213. Rambourg A, Segretain D. Three-dimensional electron microscopy of mitochondria and endoplasmic reticulum in the red muscle fiber of the rat diaphragm. *Anat Rec*. 1980;97(1):33. doi:10.1002/ar.1091970104.
214. Schlunk FF, Lombardi B, Liver liposomes I. Isolation and chemical characterization. *Lab Invest*. 1967;17:30–38.
215. Claude A. Growth and differentiation of cytoplasmic membranes in the course of lipoprotein granule synthesis in the hepatic cell. I. Elaboration of elements of the Golgi complex. *J Cell Biol*. 1970;47(3):745–766. doi:10.1083/jcb.47.3.745.
216. Wisse E, Braet F, Duime H, et al. Fixation methods for electron microscopy of human and other liver. *World J Gastroenterol*. 2010;16(23):2851–2866.doi:10.3748/wjg.v16.i23.2851.
217. Bangham AD, Horne RW. Negative staining of phospholipids and their structural modification by surface-active agents as observed in the electron microscope. *J Mol Biol*. 1964;8(5):660–668. doi:10.1016/S0022-2836(64)80115-7.
218. Bangham AD, Hill MW, Miller NGA. Preparation and use of liposomes as models of biological membranes. In: *Methods in Membrane Biology*. Vol. 1. Switzerland: Springer Nature; 1974:1–68.
219. Deeksha MM, Tewari D, Gupta G, et al. Oligonucleotide therapy: an emerging focus area for drug delivery in chronic inflammatory respiratory diseases. *Chem Biol Interact*. 2019;308:206–215. doi:10.1016/j.cbi.2019.05.028.

220. Tran -T-T, Yu H, Vidaillac C, et al. An evaluation of inhaled antibiotic liposome versus antibiotic nanoplex in controlling infection in bronchiectasis. *Int J Pharm*. 2019;559:382–392. doi:10.1016/j.ijpharm.2019.01.062.
221. Pfeiffer S, Brade L, Lindner B, et al. Localization of ceramide and glucosylceramide in human epidermis by immunogold electron microscopy. *J Invest Dermatol*. 2001;117(60):1126–1136. doi:10.1046/j.0022-202x.2001.01527.x.
222. Ploegh HL. A lipid-based model for the creation of an escape hatch from the endoplasmic reticulum. *Nature*. 2007;448(7152):435–438. doi:10.1038/nature06004.
223. Samanta S, Stiban J, Maugel TK, et al. Visualization of ceramide channels by transmission electron microscopy. *Biochim Biophys Acta*. 2011;1808 (4):1196–1201. doi:10.1016/j.bbamem.2011.01.007.
224. Siskind LJ, Kolesnick RN, Colombini M. Ceramide forms channels in mitochondrial outer membranes at physiologically relevant concentrations. *Mitochondrion*. 2006;6(3):118–125. doi:10.1016/j.mito.2006.03.002.
225. Dumas JF, Simard G, Flamment M, et al. Is skeletal muscle mitochondrial dysfunction a cause or an indirect consequence of insulin resistance in humans?. *Diabetes Metab*. 2009;35(3):159–167. doi:10.1016/j.diabet.2009.02.002.
226. Leary SC, Lyons CN, Rosenberger AG, et al. Fiber-type differences in muscle mitochondrial profiles. *Am J Physiol Regul Integr Comp Physiol*. 2003;285(4): R817–R826. doi:10.1152/ajpregu.00058.2003.
227. Ferreira R, Vitorino R, Alves RMP, et al. Subsarcolemmal and intermyofibrillar mitochondria proteome differences disclose functional specializations in skeletal muscle. *Proteomics*. 2010;10(17):3142–3315. doi:10.1002/pmic.201000173.
228. Koves TR, Noland RC, Bates AL, et al. Subsarcolemmal and intermyofibrillar mitochondria play distinct roles in regulating skeletal muscle fatty acid metabolism. *Am J Physiol Cell Physiol*. 2005;288(5):C1074–82. doi:10.1152/ajpcell.00391.2004.
229. Koves TR, Ussher JR, Noland RC, et al. Mitochondrial overload and incomplete fatty acid oxidation contribute to skeletal muscle insulin resistance. *Cell Metab*. 2008;7 (1):45–56. doi:10.1016/j.cmet.2007.10.013.
230. Debashree B, Kumar M, Keshava Prasad T, et al. Mitochondrial dysfunction in human skeletal muscle biopsies of lipid storage disorder. *J Neurochem*. 2018;145(4):323–341.228. doi:10.1111/jnc.14318.
231. Axelrod CL, Ciaran E, Fealy CE, et al. Lipids activate skeletal muscle mitochondrial fission and quality control networks to induce insulin resistance in humans. *Metabolism*. 2021;121:154803. doi:10.1016/j.metabol.2021.154803.
232. Anderson EJ, Lustig ME, Boyle KE, et al., Mitochondrial H2O2 emission and cellular redox state link excess fat intake to insulin resistance in both rodents and humans. *J Clin Invest*. 2009; 119(3): 573–581. 10.1172/JCI37048
233. Hey-Mogensen M, Jeppesen J, Madsen K, et al. Obesity augments the age-induced increase in mitochondrial capacity for H2O2 release in Zucker fatty rats. *Acta Physiol (Oxf)*. 2012;204(3):354–361. doi:10.1111/j.1748-1716.2011.02347.x.
234. Tsilingiris D, Tzeravini E, Koliaki C, et al. The role of mitochondrial adaptation and metabolic flexibility in the pathophysiology of obesity and Insulin resistance: an updated overview. *Curr Obes Rep*. 2021;10 (3):191–213.doi:10.1007/s13679-021-00434-0.
235. Perera MN, Ganesan V, Siskind LJ, et al. Ceramide channels: influence of molecular structure on channel formation in membranes. *Biochim Biophys Acta*. 2012;1818(5):1291–1301. doi:10.1016/j.bbamem.2012.02.010.
236. Ramirez T, Longato L, Dostalek M, et al. Insulin resistance, ceramide accumulation and endoplasmic reticulum stress in experimental chronic alcohol-induced steatohepatitis. *Alcohol Alcohol*. 2013;48(1):39–52. doi:10.1093/alcalc/ags106.
237. Colombini M. Ceramide channels and mitochondrial outer membrane permeability. *J Bioenerg Biomembr*. 2017;49(1):57–64. doi:10.1007/s10863-016-9646-z.
238. Becker T, Wagner R. Mitochondrial outer membrane channels: emerging diversity in transport processes. *Bioessays*. 2018;40(7):e1800013. doi:10.1002/bies.201800013.
239. Endo T, Sakaue H. Multifaceted roles of porin in mitochondrial protein and lipid transport. *Biochem Soc Trans*. 2019;47(5):1269–1277. doi:10.1042/BST20190153.
240. Krüger V, Becker T, Becker L, et al. Identification of new channels by systematic analysis of the mitochondrial outer membrane. *J Cell Biol*. 2017;216 (11):3485–3495. doi:10.1083/jcb.201706043.
241. Peterson JM, Bryner RW, Sindler A, et al. Mitochondrial apoptotic signaling is elevated in cardiac but not skeletal muscle in the obese Zucker rat and is reduced with aerobic exercise. *J Appl Physiol*. 2008. 2008;105(6):1934–1943. doi:10.1152/japplphysiol.00037.2008.
242. Petersen KF, Befroy D, Dufour S, et al. Mitochondrial dysfunction in the elderly: possible role in insulin resistance. *Science*. 2003;300(5622):1140–114219. doi:10.1126/science.1082889.
243. Davis RL, Liang C, Sue CM. Mitochondrial diseases. *Handb Clin Neurol*. 2018;147:125–141. doi:10.1016/B978-0-444-63233-3.00010-5.
244. Kyriacou K, Kassianides B, Hadjisawas A, et al. The role of electron microscopy in the diagnosis of nonneoplastic muscle diseases. *Ultrastruct Pathol*. 1997;21 (3):243–252. doi:10.3109/01913129709021920.
245. Ørngreen MC, Madsen KL, Preisler N, et al. Bezafibrate in skeletal muscle fatty acid oxidation disorders: a randomized clinical trial. *Neurology*. 2014;82(7):607–613. doi:10.1212/WNL.0000000000000118.

246. Wahwah N, Kras KA, Roust LR, et al. Subpopulation-specific differences in skeletal muscle mitochondria in humans with obesity: insights from studies employing acute nutritional and exercise stimuli. *Am J Physiol-Endocrinol Metab*. 2020;318(4):E538–E553. doi:10.1152/ajpendo.00463.2019.
247. Lowell BB, Shulman GI. Mitochondrial dysfunction and type 2 diabetes. *Science*. 2005;307(5708):384–387. doi:10.1126/science.1104343.
248. Barnett M, Collier GR, O'Dea K. The longitudinal effect of inhibiting fatty acid oxidation in diabetic rats fed a high fat diet. *Horm Metab Res*. 1992;24(8):360–362. doi:10.1055/s-2007-1003335.
249. Schmitz-Peiffer C, Browne CL, Oakes ND, et al. Alterations in the expression and cellular localization of protein kinase C isozymes epsilon and theta are associated with insulin resistance in skeletal muscle of the high-fat-fed rat. *Diabetes*. 1997;46(2):169–178. doi:10.2337/diab.46.2.169.